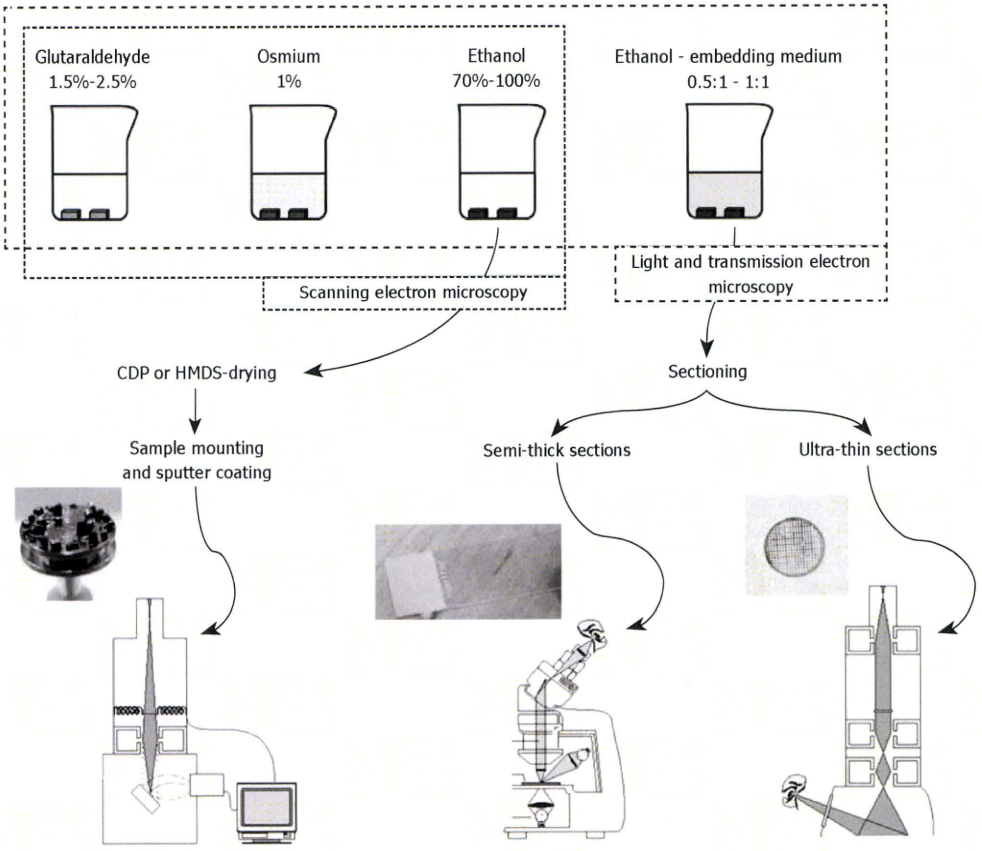

Figure 4 Summary of the different steps in the preparation of liver tissue after aldehyde fixation (top figure) and the subsequent tissue sample preparation steps for the different modes of microscopy (bottom figure). Good laboratory practice should involve all three visualization modes in order to collect fine structural and topological data, together with insights into the interior of the sample. Left: SEM; Middle: Light microscopy (LM); Right: TEM.

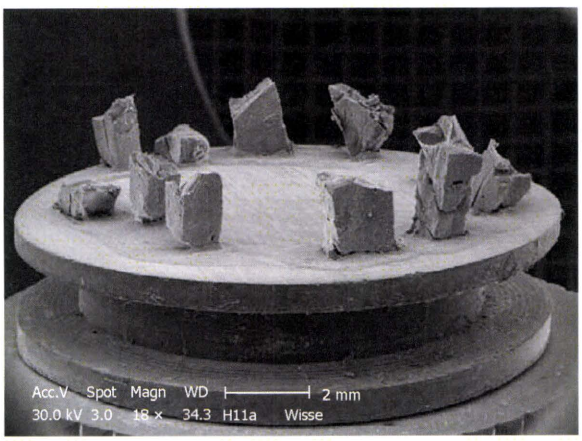

Figure 5 Typical stub of aluminum (diameter 1 cm) bearing 11 pieces of liver tissue of an injection-fixed human liver wedge biopsy observed by SEM at low magnification. Strips of tissue in 100% ethanol are frozen at -196℃, fractured, critical point dried, sputter coated and glued to this carrier. The top surface of the specimens is observed, and imaging is achieved with secondary electrons. This picture is taken by a small CCD camera fitted to the microscope to observe specimens directly.

KEY ASPECTS TO CONSIDER

Anesthesia

When using experimental animals, fixation should be preceded by anesthesia. Undoubtedly, the success of perfusion also depends on the handling of the animals. Animals should be minimally stressed before and during the operation. Therefore, it is recommended to have the animals about 2 h before the surgical procedure within the operating room to accustom them to the environment and reduce the level of stress. Stress hormones affect the physiology and fine structure of organs. Furthermore, animals in discomfort are not only difficult to manipulate, but the stress hormones might cause vasoconstriction and directly narrow or even block some vascular beds, thereby affecting the outcome of the perfusion procedure and also the fine structure of the cells.

Some researchers use ether as an anesthetic. Although this is a rapid procedure, it should be discouraged as it does not provide any pain relief, nor does it have muscle-relaxant properties. Furthermore, ether anesthesia is difficult to control, and often leads to an overdose, typically to be encountered during the initial stages of the operation, resulting in body temperature drop, shock and even accidental death of the animal. Animals that are in distress and anesthetized with ether are difficult to handle and operate on and chances for a successful liver perfusion are low. As outlined in the protocol section, agents such as pentobarbital and chloral hydrate, preferably combined with pain inhibitors, are the first-choice anesthetics. The

period of anesthesia should be as short as possible[22]. Anesthesia can be checked by gently touching the cornea of the animal, followed by gently squeezing the paw pads. When no reaction occurs, the animal is ready for operation. When laparotomy is performed, hypovolemia should be prevented and veins and arteries should be well perfused and red[22].

Preperfusion

The need for preperfusion with buffered physiological saline is still being discussed. The argument used in its favor is to wash plasma and blood cells away in order to avoid coagulation, precipitation of blood constituents and aggregation of blood cells by glutaraldehyde. Such precipitates could impair the flow of fixative through the liver. Theoretically this is correct, but experience has taught us that plasma constituents and blood cells do not have enough time to react and precipitate when glutaraldehyde is flushed through the liver straightaway. It is possible to flush the liver, e.g. of a rat, within 15-30 s without any notable obstruction. After 30 s, the way should be free to continue perfusion of the fixative. The point is that fixative and biological material need time to react, and perfusion might be successfully established before precipitation, coagulation and cellular aggregation occurs. A compromise might be to fill the tubes used for perfusion with buffered physiological saline, which results in a small "wave" of saline preceding the glutaraldehyde, the two being sequentially distributed through the entire microcirculation of the liver[22].

When preperfusion is still preferred, not more than 30 s preperfusion with buffered physiological saline at a physiological flow rate is necessary to free the liver of plasma and red blood cells. From this moment onwards, glutaraldehyde fixation can be started. The success of perfusion correlates with disappearance of red blood cells from the liver and can be followed by the change in color of the organ (dark red brown to yellow-brown). The presence of blood can also be monitored by observing the effluent. The success of fixation correlates with the change in consistency of the organ (from soft and pliable to rigid/stiff like a hard-boiled egg). Successful perfusion fixation shows the start of these phenomena within 20 to 30 s.

Air bubbles might form within the flexible tubing that connects the perfusion needle with the vessels that contain the perfusion fluids. Bubbles appear often when improperly cleaned tubing is used, or are caused by long waiting times or temperature differences between the different fluids. Air bubbles are disastrous in liver perfusion and act as blockers of the liver microcirculation. They are a major source of perfusion failure[5]. It is therefore recommended to check the tubing regularly. Air bubble traps are commercially available and are being used in clinical settings. They certainly are advised when using larger animals (e.g. rabbits, dogs or mini pigs) when high-volume perfusion is required.

As soon as perfusion is started, it is mandatory to open the vascular system by incising the vena cava in order to avoid the buildup of pressure. Enhanced pressure damages endothelial cells as well as parenchymal cells[28].

Formaldehyde has found no application in perfusion fixation of the liver. Glutaraldehyde has better stability in solution and has two reactive groups per molecule, therefore, it cross-links more easily, has lower osmotic pressure and gives better results[29]. Nevertheless, it might be useful to preperfuse the liver with formaldehyde. Since formaldehyde has a much slower reaction time than glutaraldehyde[29], it could be possible to preperfuse the liver with 3%-4% buffered (and freshly prepared) formaldehyde. Care should be taken for the high osmotic pressure of formaldehyde solutions. Formaldehyde preperfusion would allow flushing of blood and its constituents from the tissue (within 1 min) and starts mild fixation at the same time. Glutaraldehyde perfusion can be started directly thereafter and makes clear the way to do the real job of fixation in the absence of plasma and blood cells.

The choice of a roller pump *vs* gravity perfusion is a matter of personal preference. The roller pump releases moderate artery-like pulses of fluid (depending on the tube diameter), whereas gravity flow is constant and results in constant flow or pressure. The choice is considered not to be decisive for perfusion quality.

Since the liver circulation can be characterized as a high flow/low pressure system, discussions about perfusion pressure during fixation have limited value. It is believed that flow rates within wide limits do not enhance perfusion pressure, since the open system and sponge-like structure of this typical microcirculation do not allow pressure to build up. This situation changes when the fixative precipitates blood proteins, aggregates blood cells and introduces coagulation. When attention is paid to this condition, physiological flow rates (the rule of thumb: weight of liver in grams = milliliters of fluid per minute) should give good results.

Choice of the perfusion needle

Experience over the years has taught us that the outcome of fixation by perfusion also depends on the choice of the needle. The diameter of the needle, i.e. the gauge (G), determines the maximum flow to be delivered. This gauge value, together with the liver blood flow and pressure for a particular type of species, are important factors to consider. 18 G needles, for example, with a typical diameter of 1.2 mm, have a maximum perfusion flow by 12 cmH_2O gravity of 80 mL/min. This is evidently too low when livers of rabbits (177 mL/min) or dogs (303 mL/min) are concerned[30].

18-23 G needles (diameter 1.27-0.64 mm) are ideal for liver perfusion in animals such as rats and mice (Figure 1D1); whereas the 12 G (diameter 2.77 mm) needle type is recommended for larger species such as rabbits and minipigs (Figure 1D3). One can benefit from studying a catalogue of the needle catheter-type of needles that are on the market. A needle catheter (Figure 1D2) comprises a metallic needle-guide that consists of a cannula with an end grip - the catheter - that covers the needle-guide when it is retracted after cannulation. Hence, after the needle

catheter (inlet) is inserted into the portal vein and secured by ligatures, it is possible to insert the plastic tube (outlet) further into the portal vein, without rupture of the vessel. An additional benefit is that the atraumatic outlet of the catheter has a round shape, which results in more efficient perfusion when compared to the pointed-end needles. Accidental puncture of the wall of the portal vein at the start of perfusion is a major source of perfusion failure. In case of perfusion failure, an emergency solution is offered by the technique of injection fixation. In that case, the steps of protocol 2 should be followed. This might save losing an animal from the experimental setup.

A point of interest in choosing the right diameter of needle lies also in the effect of "jet streaming" that is caused by a too-small needle orifice. With an easy, moderate flow, the fluids probably distribute evenly through the branches of the portal vein, whereas a jet-stream might, simply because of its strength and direction, blow the fluids into one branch of the portal vein, thus causing uneven distribution and pressure of fixing fluids in the different liver lobes.

When injecting glutaraldehyde into a wedge biopsy, one should take care to introduce a fluid-filled needle into the tissue. When the needle cuts the tissue as it does in the case of a needle biopsy, the sampled tissue comes out at the moment the operator starts injecting the fixative. Instead, if the operator fills the needle with fluid and cuts through the tissue without allowing the tissue to enter the lumen of the needle, this effect can be avoided. Moreover, when the fluid-filled needle is retracted slightly after reaching the maximum track for injection (evidently before starting perfusion), a space will be created within the tissue, from where fluids will distribute easily in all directions as soon as the injection of the fixative solution starts.

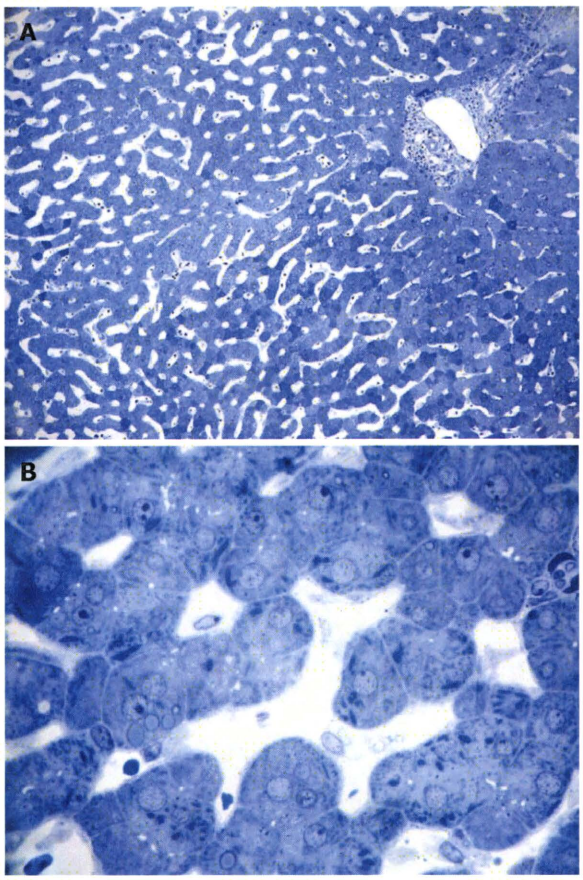

Figure 6 Light micrograph of a wedge biopsy of human liver, injected with glutaraldehyde, plastic section stained with Toluidine Blue. A: Original magnification 10 × objective lens. Note that, as a result of successful perfusion, sinusoids are open, and only a few red blood cells are present. A portal tract is present in the upper right corner; B: Original magnification 63 × oil-immersion lens. Details such as giant mitochondria are visible in the parenchymal cells, amongst others such as small mitochondria, lipid inclusions and bile canaliculi. Sinusoids are patent and show the presence of sinusoidal cells.

RESULTS OF THE DIFFERENT METHODS OF FIXATION

When LM sections, SEM preparations and ultrathin sections of liver tissue or cell cultures are studied, these three approaches provide information to the investigator, each in its own way.

Toluidine-Blue-stained 1-μm sections provide information at magnifications from 5 × to 1000 × over wide areas as compared to TEM sections (Figure 6A and B). These sections already show the criteria for good or bad fixation (see discussion), such as open sinusoids (Figure 7A and B), absence of blood cells, equal density of similar cells, and open bile canaliculi (particularly in the periportal area). Recognition of typical histological details such as the central vein, bile ducts and portal vein with its accessory structures and many cells, such as parenchymal, sinusoidal and visiting cells, together with conditions such as steatosis (Figure 8A and B), fibrosis and inflammation, can be observed at an estimated system resolution of about 0.2 μm. Crucial details such as endothelial fenestrae (measuring 140 nm in mice and rats, and 105 nm in humans and some rabbit strains) (Figures 9-12), although present, therefor escape observation by LM. Perfusion fixation and plastic embedding also add details to an LM study. In the case of immersion fixation, paraffin embedding and hematoxylin and eosin staining, observations are mainly restricted to the size, shape and position of entire cells and their nuclei. In the case of perfusion fixation and plastic embedding, intracellular details can be observed in the LM in greater detail, with the knowledge that the same structures of the same preparation can also be seen in maximal detail by TEM. For example, the typical giant mitochondria that occur in the human liver parenchymal cells (Figures 13 and 14) can easily be observed in plastic sections by LM, and can be seen in greater detail by TEM of the same specimen. Therefore, the Toluidine-Blue-stained plastic section is a useful histological introduction to further detailed study by TEM.

Perfusion-fixed total organs or injection-perfused wedge biopsies also make ideal preparations for SEM study. When tissue strips of 1 mm × 1 mm × 5 mm in 100% ethanol are frozen and fractured (before CPD) at the temperature of liquid nitrogen, the fracture surface is

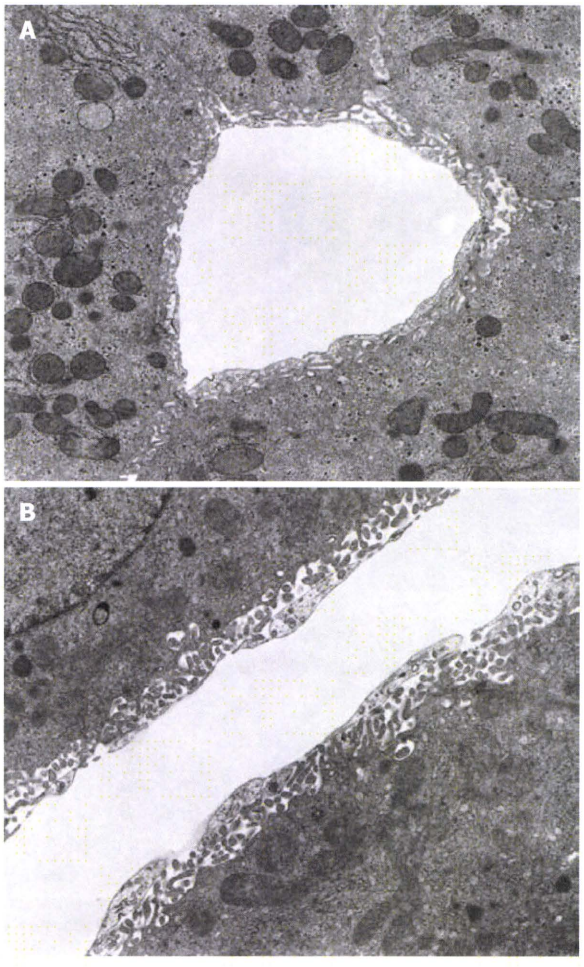

Figure 7 TEM micrograph of a transversely cut sinusoid of rabbit liver (A) and longitudinally cut sinusoid of mouse liver (B), fixed by perfusion through the portal vein. A: The Space of Disse shows the presence of microvilli extending from the parenchymal cells. Within the cytoplasm of the parenchymal cells, mitochondria, rough endoplasmic reticulum and glycogen are recognizable. Original magnification 6600 ×; B: Underneath the thin layer of fenestrated endothelium, bordering the sinusoidal lumen, the Space of Disse shows the presence of microvilli extending from the parenchymal cell surface. Within the cytoplasm of the parenchymal cells, mitochondria are recognizable. Original magnification 8900 ×.

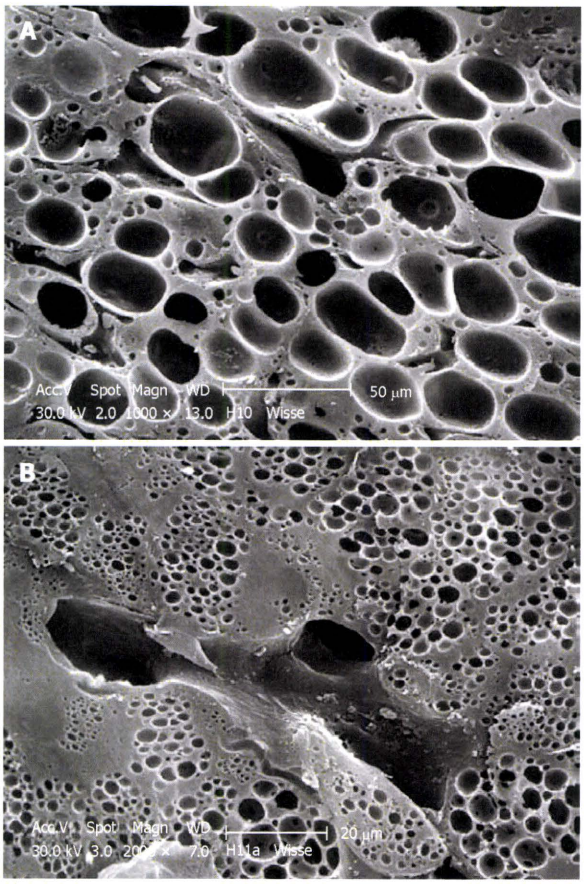

Figure 8 SEM micrograph of an injection-fixed human wedge biopsy showing macrovesicular steatosis (A) and microvesicular steatosis (B). A: Fat droplets are of such dimensions that one appears to fill the cytoplasm of an entire parenchymal cell; B: Fat droplets are smaller than those in Figure 8A and are spread within the cytoplasm of parenchymal cells.

more or less flat and easily correlates with a 2D histological section. Unfortunately, intracellular details are rare, but some cell surface details are abundant. SEM offers details about the endothelial lining of the sinusoids, easily shows the presence of fenestrae (Figures 11 and 12), reveals the presence of endothelial gaps (Figures 15 and 16), shows some details about the space of Disse, and shows the central and portal veins and the bile duct with its typical epithelial cells with one cilium each (Figure 17). Alternatively, fracturing the tissue in the already dry state after CPD (Figure 17) reveals the lateral cell membranes of parenchymal cells together with the 3D network of bile canaliculi, strictly separated from the network of sinusoids. SEM preparations are very useful in judging conditions such as sinusoidal dilatation (Figure 18) or sinusoidal obstruction syndrome[31]. Sinusoidal dilatation occurs in regions apparently different form normal, where the average sinusoidal diameter is measured as 4-6 µm by SEM. In SEM preparations, the dimensions of many structures are reduced by an average 30% shrinkage as a result of the drying procedure[23,24]. Therefore, the use of SEM preparations to measure or judge the size of any detail in the preparation should be avoided.

TEM of perfusion or injection fixed liver tissue reveals the fine structure of all the different cell types in the tissue. It is assumed that the histological topography and the shape of the cells are optimally preserved due to hardening of the intact tissue by glutaraldehyde perfusion. This initial hardening process needs only a few minutes for the entire organ. Important to note is the fact that this condition can be obtained without touching or deforming any part of the organ or tissue. It is assumed that the fluids themselves do not cause distortion as reported for immersion fixation[19].

Inherent to the observation with TEM, abundant details can be observed in all different cells and organelles at magnifications in the range of 50-1 000 000 ×, with a resolution in the order of about 5 nm. A low magnification survey of sections at 50-600 × (by using a different

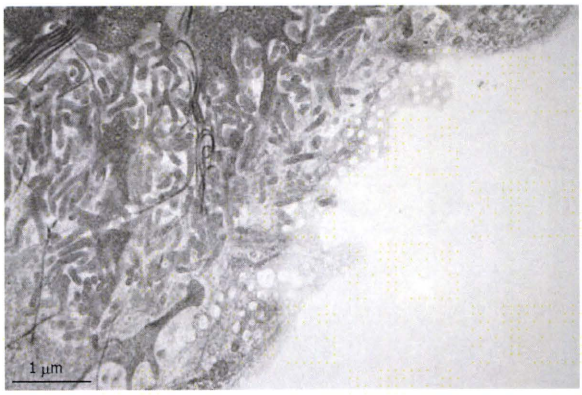

Figure 9 TEM micrograph of the tangentially cut endothelium of a human liver sinusoid, fixed by injection of glutaraldehyde fixative into a wedge biopsy. Underneath the thin layer of fenestrated endothelium, the Space of Disse shows the presence of microvilli, thin fibers of reticulin, and processes of fat-storing cells. Fenestrae in such preparations have an average diameter of about 105 nm. Original magnification 19 000 ×.

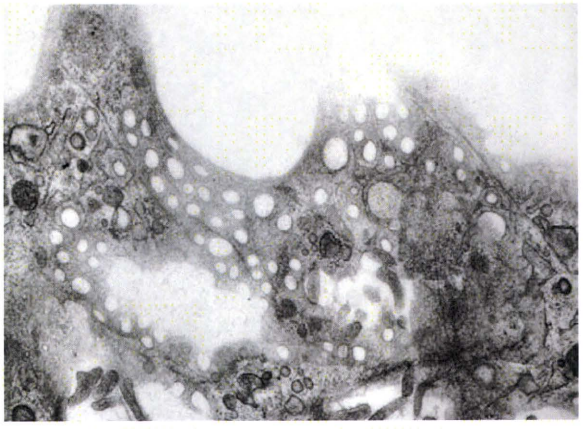

Figure 10 TEM micrograph of tangentially cut sinusoidal endothelium of a rabbit liver, fixed by perfusion through the portal vein. The fenestrae are grouped in sieve plates, but are intermingled with elements of the cytoskeleton, i.e. microtubules and microfilaments. Within the electron-dense sieve plate cytoplasm, saccular interconnecting cisternae are seen. These structures are fixation dependent and are only found in rabbit liver. Original magnification 21 000 ×.

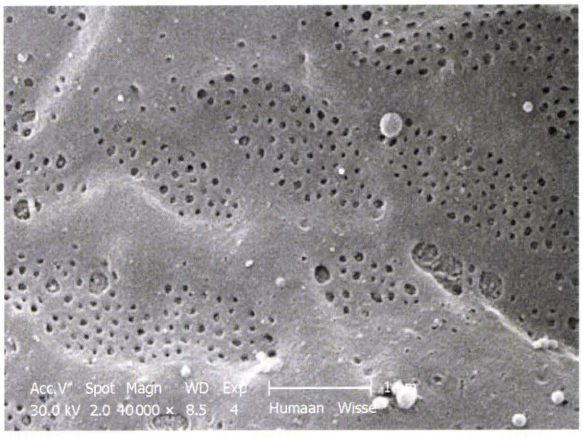

Figure 11 SEM micrograph of the fenestrated endothelial lining of a human injection-fixed wedge biopsy. Note the grouping of fenestrae in sieve plates. Compare this figure with Figure 12, which shows an SEM micrograph of a mouse sinusoid at the same magnification. Fenestrae are apparently sensitive to fixation and are lost during immersion fixation. Their presence can therefore be used as a criterion of good fixation.

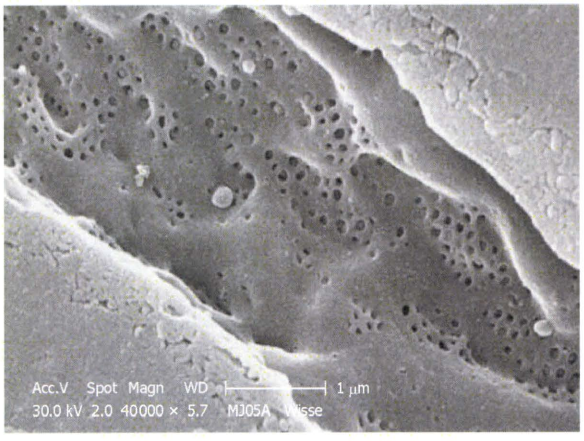

Figure 12 SEM micrograph of the fenestrated endothelial lining of a mouse portal-vein-perfused liver. Compare this figure with Figure 11, taken under exactly the same conditions. Comparison with TEM of plastic sections shows that mouse (and rat) fenestrae are bigger (140 nm) than human (and rabbit) fenestrae (105 nm). Measurements on this type of SEM preparation should be avoided, because the drying procedure results in about 30% shrinkage and incorrect measurement of all components in the tissue.

combination of TEM lenses) (Figure 19), provides information about the quality and content of the sections, and allows the preselection of interesting areas in the preparation. This low magnification TEM is also recommended as a bridge to the study of Toluidine-Blue-stained sections for LM. TEM observations also reveal the difference between sinusoids and capillaries (Figures 20 and 21). Perfusion fixation also reveals extraordinary structures such as pored domes[32] or defenestration centers (Figure 22)[33]. Higher magnifications provide supramolecular information about the cytoskeleton, glycogen rosettes, ribosomes, mitochondrial cristae, chromatin fine structure, nucleolar composition, unit membrane structure, Golgi apparatus, the presence of iron storage proteins, and lysosomal contents.

Results obtained with cell cultures follow the general pattern described for the three kinds of specimen already discussed. In the case of cultured cells, fixation at the cellular level is quite easy. A big difference is that fluids have direct access to the cells. Therefore, precautions should be taken to avoid over-fixation and extraction, which can result in damaged membranes and extracted cells.

GENERAL DISCUSSION

A detailed literature survey has revealed that there are three commonly used fixation methods for EM studies of liver tissue. For a review see Hayat[21]. Since Fahimi[5] and Wisse[6] have demonstrated that perfusion fixation, rather than immersion fixation, is essential in preserving the fine structure and architecture of the liver, perfusion-fixation has been the gold standard ever since, especially

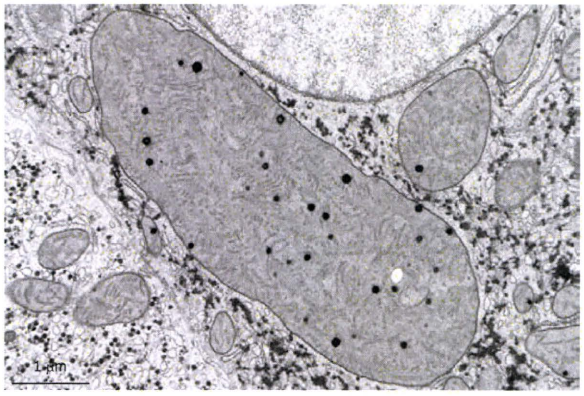

Figure 13 Typical structures that are often encountered in human liver parenchymal cells are the giant mitochondria. This wedge biopsy was fixed by injection, but during the osmium postfixation, ferrocyanide has been added. This compound enhances the contrast of membranes, including the cristae. Giant mitochondria also contain electron-dense granules, as normally seen in small mitochondria (compare Figure 14). Giant mitochondria can also be recognized in plastic sections observed by LM (see Figure 6B). Magnification 19000 ×.

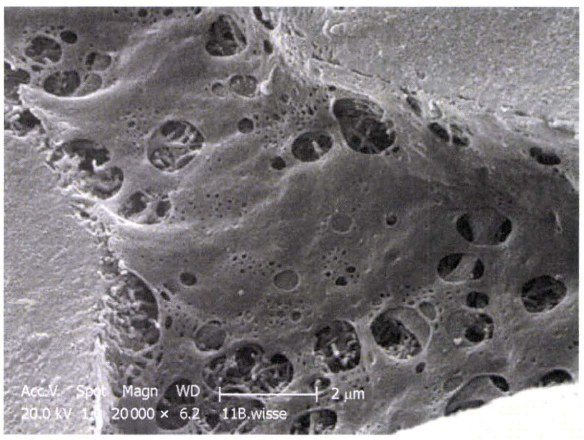

Figure 15 A major problem in EM preparations of liver tissue is the occurrence of gaps in the endothelial lining. It is assumed that they appear during fixation due to instability of the cytoskeleton, which allows the fusion of fenestrae or the *de novo* formation of gaps. This SEM picture is from a rabbit liver fixed by portal perfusion.

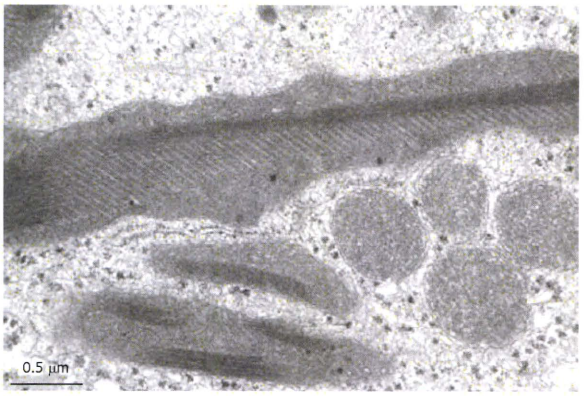

Figure 14 Giant mitochondria in a wedge biopsy fixed by injection. No ferrocyanide has been added during the osmium postfixation, therefore, membrane contrast is low. Within the giant mitochondria, the occurrence of typical crystals can be observed, together with a highly rhythmical pattern of the cristae. Magnification 34000 ×.

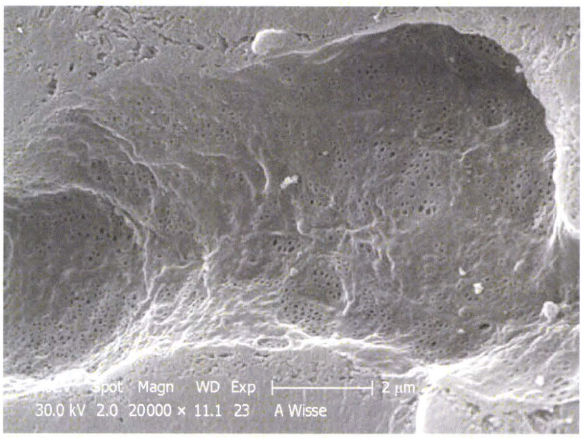

Figure 16 SEM micrograph of another portal-vein-perfused rabbit liver, which shows a complete intact sinusoid, and apparently no gaps have been formed. Fenestrae occur in sieve plates (groups), the space of Disse seems to be filled by microvilli of the parenchymal cells.

for the study of the sinusoids and sinusoidal cells in experimental animals[6].

Irrespective of the numerous methods available to prepare liver tissue for EM studies, perfusion-fixation *via* the portal vein is decidedly superior and more reproducible compared to other methods of fixation, in particular immersion fixation. Injection of the fixative into wedge biopsies, however, comes close and when Toluidine-Blue-stained LM sections are used to select tissue for the quality of fixation, this type of fixation can replace that through the portal vein. Perfusion-fixation *via* the portal vein and immediate arrest of the liver circulation (including the hepatic artery), meets the conditions of instantaneous and simultaneous fixation of all cells in the organ and restricts gradients of fixation to the cellular level. Fahimi[5] and Wisse *et al*[22] have reported the success of portal vein perfusion, followed by retrograde perfusion with fixative through the hepatic vein, which results in more evenly fixed tissue. By staining with Schiff's reagent, we could demonstrate that within 5-7 min, liver tissue stains equally well after such "push-pull" fixation[22], which indicates that saturation of the tissue with glutaraldehyde is obtained over this short time interval. Perfusion through the aorta[28] or any other indirect route may be successful, but seems unnecessary when the portal vein is available. We can summarize the advantages of perfusion fixation as follows: (1) instantaneous and simultaneous fixation of all cells in the organ; (2) avoidance of hypoxia and autolysis; (3) fewer problems resulting from diffusion and exhaustion of the fixative during immersion; (4) use of lower concentrations of fixing chemicals is possible; (5) glutaraldehyde perfusion hardens the tissue, which allows easier cutting; (6) less mechanical damage, deformation or distortion; (7) empty vessels and sinusoids allow better penetration of

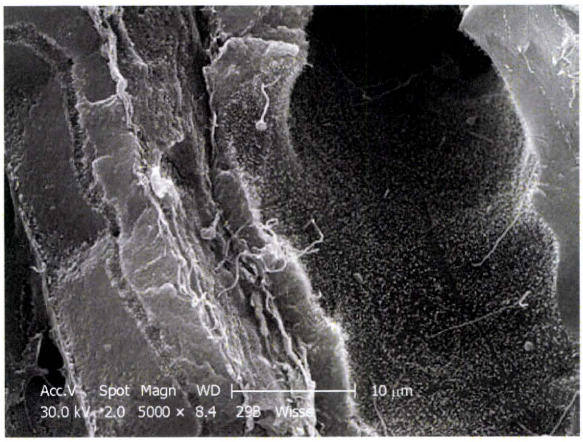

Figure 17 SEM micrograph of rabbit liver, fractured after CPD. In such preparations, the fracture plane separates the intact lateral cell membranes of parenchymal cells, which exposes the bile canaliculi, which are strictly separated from the sinusoids (to the extreme left). The right hand side of the picture shows a bile duct. The luminal surface of the bile duct epithelial cells is covered with numerous small microvilli and single cilia protruding into the lumen of the bile duct.

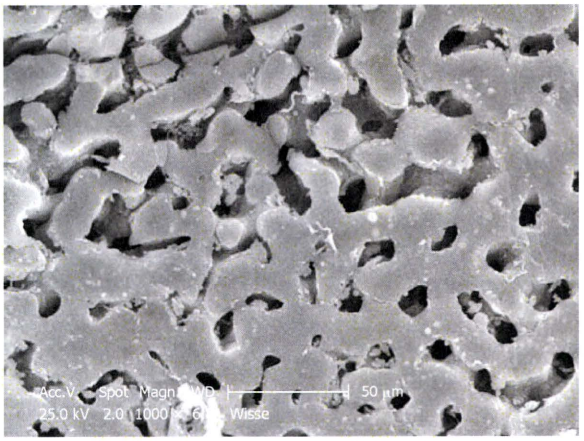

Figure 18 SEM micrograph of a human injection-fixed wedge biopsy that shows two populations of sinusoids, i.e. normal size (lower half of the picture), and those in the upper half of the picture show sinusoidal dilatation.

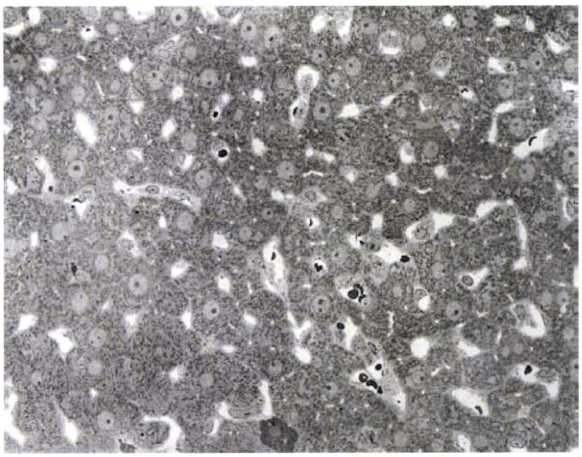

Figure 19 TEM image after perfusion fixation of rat liver through the portal vein, which results in an image of parenchymal cells of equal density (with one exception in the low middle part), open sinusoids and open bile capillaries. Original magnification 720 ×.

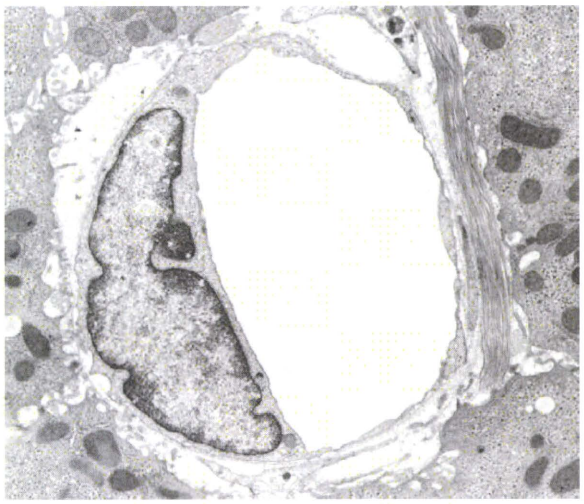

Figure 20 TEM micrograph of a capillary found in diseased human liver, fixed by injection of fixative into a wedge biopsy. Capillary endothelial cells are different from normal sinusoidal endothelial cells; their vacuolar apparatus (pinocytotic vesicles, endosomes, lysosomes, Golgi apparatus) is not developed. The thin cytoplasm contains fenestrae and the capillary is surrounded by a thin, continuous basal lamina that is not present in normal sinusoids. Magnification 6600 ×.

washing fluids, osmium and ethanol; (8) exact timing and shorter fixation times are possible; (9) more and better preservation of histological relationships and fine structural details; (10) better preservation of cytochemical reactive sites; (11) fewer artifacts; (12) perfusion can be extended to a program of reagents, fixatives and buffers without further manipulation; (13) less accessible organs and tissues may be fixed before excision; and (14) easy to directly judge good perfusion and fixation by change in color and hardening of the organ.

An additional advantage of the method is that perfusion-fixed liver tissue is firm enough to be cut into finer pieces without deformation, supposedly leaving cells in their right histological arrangement. Hand cutting by a sharp, thin razor blade allows the cutting of glutaraldehyde fixed tissue into tissue blocks of 1 mm × 1 mm × 1 mm (for TEM) or slices (1 mm × 10 mm × 10 mm) for flat embedding and large sections for LM, and strips of 1 mm × 1 mm × 5 mm for further preparation for SEM. It is assumed that the open vessels and sinusoids allow the penetration of osmium and other fluids in a much better way as compared to immersion fixation, for which a wall of fixed components at the outer rim of the tissue stands in the way of and will still react with the penetrating fluid.

Researchers may choose from two perfusion methods that both result in excellent preservation of hepatic tissue. One uses gravity to perfuse the vascular bed at 12 cm water pressure, a value that corresponds to the physiological portal pressure (Figure 1A); whereas the other method actively pumps solutions through the portal vein with the

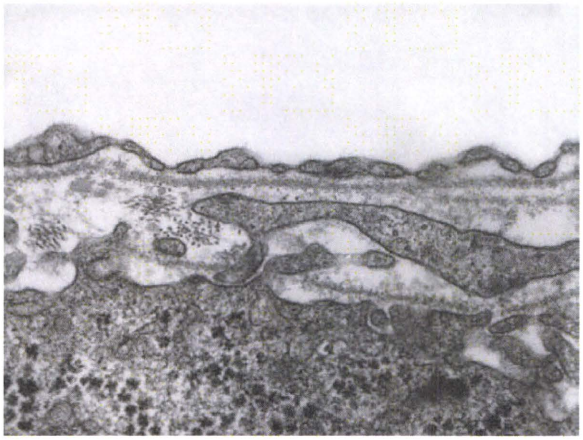

Figure 21 TEM micrograph of a capillary found in diseased human liver, fixed by injection of fixative into a wedge biopsy. The thin endothelial lining contains fenestrae, closed by a diaphragm. Underneath the endothelium, one can observe a continuous basal lamina. Fenestrae in this type of capillary are about 60 nm in diameter. It is supposed that transport from this capillary to the tissue is hampered by the structures mentioned. Magnification 28 500 ×.

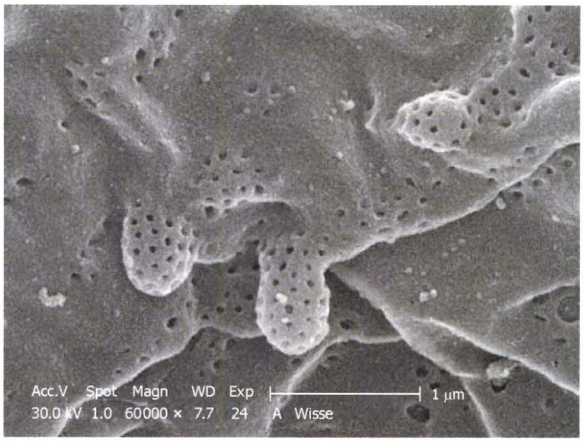

Figure 22 SEM micrograph of a portal-vein-perfused rabbit liver. Due to the quality of fixation, fenestrae are preserved, including a surprising detail, named pored domes[32], which are probably the *in vivo* equivalent of the defenestration center observed in endothelial cell cultures[33]. This structure was not seen in human, mouse, rat or pig liver.

aid of a low-speed peristaltic pump. In both cases the typical rate of 1 mL/min per g liver weight (Figure 1B) should be achieved.

Perfusion fixation seems to be difficult when a human needle biopsy is to be investigated by EM. Attempts have been made by Bioulac-Sage *et al*[14] and Balabaud *et al*[8] to flush fluids through the tissue of a liver needle biopsy arrested at one end of a narrowing Pasteur pipette (holding the tissue) with a slightly elevated pressure, while aspirating fluids at the other end with slightly negative pressure. Muto *et al*[10], Vonnahme[12] and De Wilde *et al*[15] have obtained good fixation results on human or rat liver needle biopsies by injecting glutaraldehyde with tiny glass or metal needles at intervals into the cylindrical tissue. De Wilde *et al*[15] have used low-melting-point agar to arrest and handle the tissue. Surprisingly, and in spite of good results, this technique has not found its way into clinical practice, and it is not mentioned in the needle biopsy review of Rockey *et al*[3].

It is evident that immersion-fixed needle biopsies have provided a wealth of information about the fine structure and deviations of parenchymal cells. David *et al*[34] have demonstrated by morphometric methods that there are only slight differences between parenchymal cells from immersion- or perfusion-fixed tissue. It is recommended to limit the study of immersion-fixed needle biopsies to the outer and middle zone of cells that are well fixed. They can easily be found when material is preselected by Toluidine-Blue-stained LM sections. Apparently, the structure of sinusoids and sinusoidal cells, as damaged as they are after immersion fixation, has not until now played a significant role in clinical practice.

With regard to artifacts, we remember a citation from one of the founding fathers of EM, George Palade, who said that one of the major difficulties in EM is to distinguish between genuine structures and artifacts. Some even say that EM is "an art of artifacts". It takes indeed a lot of experience and insight to distinguish between real structures and artifacts. Alternative methods are scarce, but sometimes it helps to compare results of chemical fixation (as summarized in this review) with alternative techniques such as freeze fracture of fresh tissue[6]. In equilibrium with the fact that artifacts are not easy to define and to prove, it is also difficult to indicate the true nature of real structures and their function. Artifacts in a specimen can be caused during one or more of the many steps of sample preparation, and can be caused by anesthesia, osmotic pressure, quality of the reagents, inadequate operation, pH, temperature, postmortem changes or autolysis, slow or incomplete fixation, cutting of the tissue, postfixation, dehydration, distortion, embedding, sectioning, contrast staining, microscope conditions, (digital) photography, image storage, and handling. Examples of possible artifacts are the occurrence of endothelial gaps, shrunken cells, light cells next to dark cells (Figure 23), widening of the Space of Disse, changes in cell shape, changes in the rounded shape of the nucleus of the parenchymal cells, condensation of chromatin[19], relocation or disappearance of subcellular components (such as endothelial fenestrae[6]), swollen mitochondria, collapsing and blebbing (Figure 24) of cell membranes and vesicle formation in intercellular spaces.

With regard to the occurrence of gaps larger than fenestrae in the endothelial lining (Figure 15) a lot of discussion has taken place[22,23]. Indirect proof of their artifactual nature is given by the fact that, in intact animals, endothelial fenestrae have an apparent sieving effect on, for example, adenoviral vectors of 93 nm used for gene transfer[35,36]. The appearance of large gaps in the sinusoidal lining can result from osmolarity problems, from destabilization of the cytoskeleton or from the use of a high perfusion pressure during the washing and subsequent glutaraldehyde fixation during the perfusion-fixation procedures[28,34].

Other subtle artifacts are caused by a process often

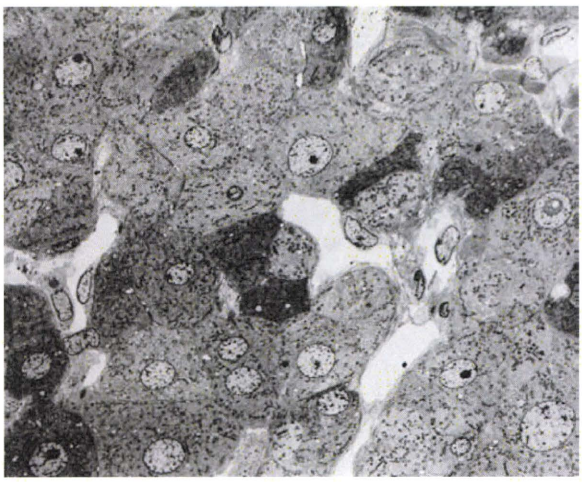

Figure 23 TEM micrograph of an injection-fixed human liver wedge biopsy at 700 × magnification, which shows the presence of dark and light cells next to each other. It is assumed that the differences in density reflect differences in fixation, which often occur in bad fixation.

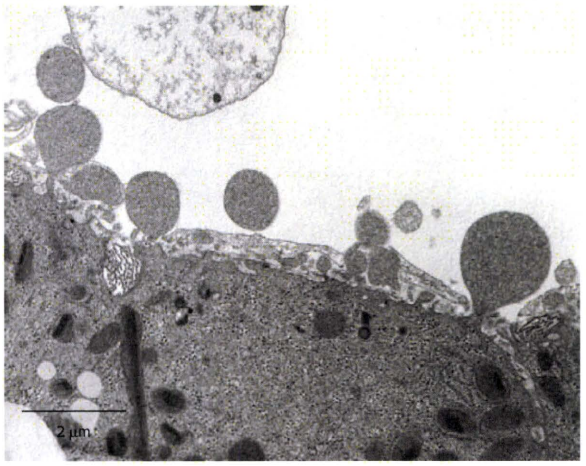

Figure 24 TEM micrograph of an injection-fixed human liver wedge biopsy, which shows the presence of blebbing, which occurs when cells survive in bad conditions. Incomplete fixation is thought to be the cause. Blebs are either swollen microvilli or originate from the peripheral cytoplasm of parenchymal cells. Original magnification 7900 ×.

referred to as over-fixation or "weekend fixation". People sometimes store their precious samples for hours, days or even weeks in glutaraldehyde fixative. Typical for those preparations is that they are rich in free vesicles that seem to form from loose phospholipids derived from the cell membrane. Conversely, blebbing of living parenchymal cells occurs at low oxygen and glutaraldehyde concentrations (Figure 24). Related to this is the clumping of individual glycogen inclusions, poorly staining cell membranes, and failure to achieve staining of glycogen in parenchymal cells. With regard to the transport of material between laboratories, we have good experience of sending samples in 70% ethanol by fast courier services, which are able to deliver between different continents within 1 or 2 d.

How does one assess the outcome of properly fixed liver tissue? In order to distinguish good quality of fixation of the liver, we recommend the following criteria: (1) sinusoids should be open; (2) plasma and blood cells should be practically absent in sinusoids; (3) similar cell types should show similar images; (4) endothelial fenestrae should be present; (5) bile canaliculi (especially in the periportal area) should be open[6,8,22,23]; and (6) nuclei of parenchymal cells should be round (When nuclei of parenchymal cells are elliptic, the nuclei are compressed in the direction of cutting in the ultramicrotome).

The following criteria can be use to distinguish bad fixation: (1) sinusoids are collapsed or largely destructed and still filled with plasma and blood cells; (2) dark and light cells occur next to each other; (3) different images of similar cells; (4) endothelial fenestrae are absent; (5) bile canaliculi are collapsed; and (6) irregularly shaped nuclei of parenchymal cells.

Fahimi[5] has immersed thin slices of perfusion-fixed liver tissue into distilled water. When they change to a white color, the fixation is insufficient. This is a simple, rapid and objective test for good fixation.

Although this paper focuses mainly on the study of ultrathin liver sections with TEM, SEM is also a powerful tool to assess the quality of perfusion-fixed liver tissue. The abundant presence of red blood cells within sinusoids is an indicator of improper perfusion. Sometimes investigators unwarily apply unrelated or unsuitable perfusion or fixation procedures that are fine-tuned for specific applications, tissues, species or even are not applicable for animal tissue material, such as microbial and plant sample preparation protocols. Animal tissue and their cell components have a typical osmotic pressure of 320 mOsmol. Since the osmolarity of the glutaraldehyde component of the fixative seems to be less important[19,37], the osmolarity of the buffers should match the osmotic values of the tissue. Isotonic solutions that include the osmotic pressure of glutaraldehyde have a swelling effect on cells[37]. The protocols described in this review have contributed to the success of EM studies in several groups. The composition of the fluids applied reports the use of sucrose, which is added to a 0.1 mol/L sodium cacodylate buffer to correct its osmotic value to 320 mOsmol.

In vitro perfusion of whole livers has been used often to study preservation conditions of livers for transplantation, or metabolic and physiological processes. It is important to note that perfusion fixation fits well into such schemes and provides essential information about the condition of those livers at the end of an experiment. In addition, perfusion can also be used to incubate the tissue for cytochemical reactions of enzymes, epitopes, and all other reactive elements within the tissue.

CONCLUSION

In a clinical environment, the immersion-fixed needle biopsy is an important standard. The role of needle biopsies in diagnosis, prognosis and management of patients with liver disease[3] makes the needle biopsy a gold standard,

notwithstanding immersion fixation, paraffin embedding, thick 5-μm sections, and the use of low-magnification LM. Together with immunological techniques, specific staining and the professional training of pathologists, needle biopsies fulfill clinical needs. Pathological diagnosis[38] uses pattern recognition in tissues that reveal conditions such as steatosis, inflammation, hyperplasia and neoplasia. EM seems to be of limited or no use in diagnosis[3], in contrast to its use in research. However, EM still has a potential value in a clinical environment.

However, at the other end of the spectrum, there is a group of scientists that knows that perfusion fixation, plastic embedding and the use of EM provides details about cells and tissues down to the nanometer level. Surprisingly, EM does not seem to succeed in helping pathologists to improve further their diagnosis with data derived at this supramolecular level. One of the key elements in this process is, according to the present authors, the lack of use of perfusion fixation for the study of liver tissue from patients. Indeed, we suppose that applying this type of fixation will provide evidence that might be used to the advantage of patients, for understanding the pathogenesis of certain diseases. This was the motivation for writing this review; to summarize the techniques and bring them to the attention of those involved in the process of using microscopic observations to support diagnosis and prognosis of liver diseases. There seems to be a gap between the use of low-resolution LM observations on immersion-fixed, paraffin-embedded, 5-μm sections and high-resolution microscopy of perfusion-fixed tissue. We hope that this review might help to bridge that gap. Essential to this approach is the recognition of the fact that liver tissue should be fixed at the cellular level with fluids that are as close to physiological and physical conditions as possible.

A good fundamental knowledge of the fine structure and histology of the normal liver is needed because some experimental conditions, pathological processes and severe liver diseases result in outcomes comparable to bad fixation. Although it is difficult to decide between genuine and artifactual structures in normal liver, the decision becomes even more difficult when disease conditions are added to the process.

REFERENCES

1 **Geuze HJ**. A future for electron microscopy in cell biology? *Trends Cell Biol* 1999; **9**: 92-93
2 **Braet F**, Ratinac K. Creating next-generation microscopists: structural and molecular biology at the crossroads. *J Cell Mol Med* 2007; **11**: 759-763
3 **Rockey DC**, Caldwell SH, Goodman ZD, Nelson RC, Smith AD. Liver biopsy. *Hepatology* 2009; **49**: 1017-1044
4 **Claude A**, Fullam EF. The preparation of sections of guinea pig liver for electron microscopy. *J Exp Med* 1946; **83**: 499-503
5 **Fahimi HD**. Perfusion and immersion fixation of rat liver with glutaraldehyde. *Lab Invest* 1967; **16**: 736-750
6 **Wisse E**. An electron microscopic study of the fenestrated endothelial lining of rat liver sinusoids. *J Ultrastruct Res* 1970; **31**: 125-150
7 **Bhatnagar MK**, David LL, Vrablic O, Therien A, Blouin A. A simple method for perfusion fixation of avian liver for electron microscopy. *Can J Zool* 1981; **59**: 1179-1183
8 **Balabaud C**, Boulard A, Quinton A, Saric J, Bedin C, Boussarie L, Bioulac-Sage P. Light and transmission electron microscopy of sinusoids in human liver. In: Bioulac-Sage P, Balabaud C, editors. Sinusoids in human liver: health and disease. Rijswijk: The Kupffer Cell Foundation, 1988: 87-110
9 **Burwen SJ**, Jones AL, Goldman IS, Way LW, Dejbakhsh S. The perfused human liver wedge biopsy: a new in vitro model for morphological and functional studies. *Hepatology* 1982; **2**: 426-432
10 **Muto M**, Nishi M, Fujita T. Scanning electron microscopy of human liver sinusoids. *Arch Histol Jpn* 1977; **40**: 137-151
11 **Sandström B**. Liver fixation for electron microscopy by means of transparenchymal perfusion with glutaraldehyde. *Lab Invest* 1970; **23**: 71-73
12 **Vonnahme FJ**. An improved method for transparenchymal fixation of human liver biopsies for scanning electron microscopy. *Scan Electron Microsc* 1980; 177-180
13 **Wisse E**, Jacobs F, Topal B, Frederik P, De Geest B. The size of endothelial fenestrae in human liver sinusoids: implications for hepatocyte-directed gene transfer. *Gene Ther* 2008; **15**: 1193-1199
14 **Bioulac-Sage P**, Lamouliatte H, Saric J, Balabaud C. [Perfusion-fixation of liver needle biopsy: technic] *Gastroenterol Clin Biol* 1984; **8**: 656-659
15 **De Wilde A**, Van Der Spek P, Devis G, Wisse E. On the fixation of needle biopsies of rat liver tissue as a model to study the fine structure of sinusoidal cells. In: Knook DL, Wisse E, editors. Sinusoidal Liver Cells. Rijswijk: The Kupffer Cell Foundation, 1982: 85-92
16 **Horn T**, Christoffersen P. Perfusion fixation of hepatic needle biopsies for scanning electron microscopy. A methodological study. *Liver* 1986; **6**: 89-97
17 **Gendrault JL**, Montecino-Rodriguez F, Cinqualbre J. Structure of the normal human liver sinusoid after perfusion fixation. In: Knook DL, Wisse E, editors. Sinusoidal Liver Cells. Amsterdam: Elsevier/North-Holland Biomedical Press, 1982: 93-100
18 **Wisse E**, De Wilde A, De Zanger R. Perfusion fixation of human and rat liver tissue for light and electron microscopy: a review and assessment of existing methods with special emphasis on sinusoidal cells and microcirculation. In: O'Hare AMF, editor. Science of Biological Specimen Preparation. Chicago: SEM Inc., 1984: 31-38
19 **Bullock GR**. The currejnt status of fixation for electron microscopy: a review. *J Microscopy* 1984; **133**: 1-15
20 **White DL**, Mazurkiewicz JE, Barrnett RJ. A chemical mechanism for tissue staining by osmium tetroxide-ferrocyanide mixtures. *J Histochem Cytochem* 1979; **27**: 1084-1091
21 **Hayat MA**. Principles and techniques of electron microscopy: biological applications. Cambridge: Cambridge University Press, 2000
22 **Wisse E**, De Zanger RB, Jacobs R, McCuskey RS. Scanning electron microscope observations on the structure of portal veins, sinusoids and central veins in rat liver. *Scan Electron Microsc* 1983; 1441-1452
23 **Wisse E**, De Zanger RB, Charels K, Van Der Smissen P, McCuskey RS. The liver sieve: considerations concerning the structure and function of endothelial fenestrae, the sinusoidal wall and the space of Disse. *Hepatology* 1985; **5**: 683-692
24 **Boyde A**, Wood C. Preparation of animal tissues for surface-scanning electron microscopy. *J Microsc* 1969; **90**: 221-249
25 **Nation JL**. A new method using hexamethyldisilazane for preparation of soft insect tissues for scanning electron microscopy. *Stain Technol* 1983; **58**: 347-351
26 **Boyde A**. Review of basic preparation techniques for biological scanning electron microscopy. In: Brederoo P, de Priester W, editors. Electron microscopy. The Hague: 7th Eur. Congress Electron Microsc Foundation Leiden, 1980: 768-777
27 **Braet F**, De Zanger R, Wisse E. Drying cells for SEM, AFM

and TEM by hexamethyldisilazane: a study on hepatic endothelial cells. *J Microsc* 1997; **186**: 84-87
28 **Frenzel H**, Kremer B, Richter IE, Hücker H. [The fine structure of liver sinusoids after perfusion fixation with various pressures. A transmission and scanning electron microscopic study (author's transl)] *Res Exp Med* (Berl) 1976; **168**: 229-241
29 **Fox CH**, Johnson FB, Whiting J, Roller PP. Formaldehyde fixation. *J Histochem Cytochem* 1985; **33**: 845-853
30 **Davies B**, Morris T. Physiological parameters in laboratory animals and humans. *Pharm Res* 1993; **10**: 1093-1095
31 **DeLeve LD**. Hepatic microvasculature in liver injury. *Semin Liver Dis* 2007; **27**: 390-400
32 **Tanuma Y**, Ohata M, Ito T. A transmission electron microscopic study of rabbit liver sinusoids with special remarks on an experimentally induced canalicular system and the "pored domes" in the endothelial cells. *Arch Histol Jpn* 1987; **50**: 177-192
33 **Braet F**, Muller M, Vekemans K, Wisse E, Le Couteur DG. Antimycin A-induced defenestration in rat hepatic sinusoidal endothelial cells. *Hepatology* 2003; **38**: 394-402
34 **David H**, Uerlings I. Quantitative ultrastructure of the rat liver by immersion and perfusion fixations. *Exp Pathol* 1983; **23**: 131-141
35 **Lievens J**, Snoeys J, Vekemans K, Van Linthout S, de Zanger R, Collen D, Wisse E, De Geest B. The size of sinusoidal fenestrae is a critical determinant of hepatocyte transduction after adenoviral gene transfer. *Gene Ther* 2004; **11**: 1523-1531
36 **Snoeys J**, Lievens J, Wisse E, Jacobs F, Duimel H, Collen D, Frederik P, De Geest B. Species differences in transgene DNA uptake in hepatocytes after adenoviral transfer correlate with the size of endothelial fenestrae. *Gene Ther* 2007; **14**: 604-612
37 **Arborgh B**, Bell P, Brunk U, Collins VP. The osmotic effect of glutaraldehyde during fixation. A transmission electron microscopy, scanning electron microscopy and cytochemical study. *J Ultrastruct Res* 1976; **56**: 339-350
38 **Desmet VJ**. The amazing universe of hepatic microstructure. *Hepatology* 2009; **50**: 333-344

S- Editor Tian L **L- Editor** Kerr C **E- Editor** Lin YP

0090-9556/10/3811-1954–1961$20.00
DRUG METABOLISM AND DISPOSITION

DMD 38:1954–1961, 2010

Vol. 38, No. 11
31732/3633215
Printed in U.S.A.

Effect of Hepatitis C Virus Infection on the mRNA Expression of Drug Transporters and Cytochrome P450 Enzymes in Chimeric Mice with Humanized Liver[S]

Ryota Kikuchi, Matthew McCown, Pamela Olson, Chise Tateno, Yoshio Morikawa, Yumiko Katoh, David L. Bourdet, Mario Monshouwer, and Adrian J. Fretland

Non Clinical Safety, Department of Drug Metabolism and Pharmacokinetics (R.K., D.L.B., M.Mo., A.J.F.), Viral Disease Biology Area (M.Mc.), and Molecular Medicine Laboratories (P.O.), Roche Palo Alto, Palo Alto, California; and PhoenixBio Co., Ltd., Higashi-Hiroshima, Japan (C.T., Y.M., Y.K.)

Received December 16, 2009; accepted August 6, 2010

ABSTRACT:

The expression of drug transporters and metabolizing enzymes is a primary determinant of drug disposition. Chimeric mice with humanized liver, including PXB mice, are an available model that is permissive to the in vivo infection of hepatitis C virus (HCV), thus being a promising tool for investigational studies in development of new antiviral molecules. To investigate the potential of HCV infection to alter the pharmacokinetics of small molecule antiviral therapeutic agents in PXB mice, we have comprehensively determined the mRNA expression profiles of human ATP-binding cassette (ABC) transporters, solute carrier (SLC) transporters, and cytochrome P450 (P450) enzymes in the livers of these mice under noninfected and HCV-infected conditions. Infection of PXB mice with HCV resulted in an increase in the mRNA expression levels of a series of interferon-stimulated genes in the liver. For the majority of genes involved in drug disposition, minor differences in the mRNA expression of ABC and SLC transporters as well as P450s between the noninfected and HCV-infected groups were observed. The exceptions were statistically significantly higher expression of multidrug resistance-associated protein 4 and organic anion-transporting polypeptide 2B1 and lower expression of organic cation transporter 1 and CYP2D6 in HCV-infected mice. Furthermore, the enzymatic activities of the major human P450s were, in general, comparable in the two experimental groups. These data suggest that the pharmacokinetic properties of small molecule antiviral therapies in HCV-infected PXB mice are likely to be similar to those in noninfected PXB mice. However, caution is needed in the translation of this relationship to HCV-infected patients as the PXB mouse model does not accurately reflect the pathology of patients with chronic HCV infection.

Introduction

Elimination of endogenous and exogenous substances is one of the most important physiological functions of the liver, which comprises the sinusoidal uptake from the blood circulation, intracellular phase I and phase II metabolism, and canalicular efflux of parent compound and/or metabolites into bile. Cumulative evidence suggests that members of the solute carrier (SLC) and ATP-binding cassette (ABC) transporters are expressed on either sinusoidal or canalicular membrane of the hepatocytes where they are responsible for the sinusoidal uptake and bile canalicular efflux of a diverse set of compounds (Chandra and Brouwer, 2004; Shitara et al., 2006; Dobson and Kell, 2008). On the other hand, cytochrome P450 enzymes are localized to the endoplasmic reticulum of hepatocytes and are the major enzymes involved in phase I drug metabolism and bioactivation, accounting for approximately 75% of the oxidative metabolism of marketed drugs (Gonzalez, 1990; Rendic and Di Carlo, 1997). Other enzymes such as glutathione transferase, UDP-glucuronosyltransferase, and sulfotransferase are involved in the conjugation of xenobiotics in phase II metabolism (Meyer, 1996; Williams et al., 2004). The expression and function of these transporters and enzymes are important determinants of the physiological turnover of endogenous compounds and clearance of exogenous substances including clinically used drugs.

Hepatitis C virus (HCV) infects an estimated 170 million people worldwide, and its infection is a leading cause of chronic hepatitis, liver cirrhosis, and hepatocellular carcinoma (World Health Organization, 1999). Currently, the combination therapy of pegylated interferon (IFN) and ribavirin is the only approved treatment for HCV infection. However, this treatment regimen is only effective in ap-

Article, publication date, and citation information can be found at http://dmd.aspetjournals.org.
doi:10.1124/dmd.109.031732.
[S] The online version of this article (available at http://dmd.aspetjournals.org) contains supplemental material.

ABBREVIATIONS: SLC, solute carrier; ABC, ATP-binding cassette; HCV, hepatitis C virus; IFN, interferon; uPA/SCID, urokinase plasminogen activator-transgenic severe combined immunodeficiency disorder; PCR, polymerase chain reaction; ISG, interferon-stimulated gene; hGAPDH, human glyceraldehyde-3-phosphate dehydrogenase; P450, cytochrome P450; LC, liquid chromatography; MS/MS, tandem mass spectrometry; MRP, multidrug resistance-associated protein; OATP, organic anion-transporting polypeptide; OCT, organic cation transporter; P-gp, P-glycoprotein; MDR, multidrug resistance; BSEP, bile salt export pump; NTCP, Na^+-taurocholate cotransporting polypeptide; OAT, organic ion transporter; C_t, cycle threshold.

proximately 50% of all patients infected with HCV. A number of individuals with HCV infection are unable to achieve a sustained virological response with the current therapy, and many of them will progress to liver diseases resulting from chronic infection with HCV. Thus, the development of more efficient therapies against HCV is of high priority (Wakita, 2007).

Several in vitro experimental models have been used to investigate the pathology of HCV as well as the efficacy of potential therapeutic compounds. These models include the use of individually cloned proteins of HCV (Littlejohn et al., 1998), infection of primary culture human hepatocytes with HCV (Buck, 2008), and in vitro HCV replicon systems in Huh-7 cells (Bartenschlager, 2005). The HCV replicon systems are particularly useful in HCV research and drug discovery because they are both permissive to high-efficiency HCV replication and respond to antiviral compounds including IFN-α and ribavirin. However, several limitations exist with the use of replicon systems in the discovery and development of novel anti-HCV compounds. These include the cell culture-adaptive mutations of the HCV genome and the innate difference of Huh-7 cells, which are immortalized tumor cells, compared with hepatocytes.

Because of the strict tropism of HCV, only humans and higher primates, such as chimpanzees, have, until recently, been receptive to authentic HCV infection and the development of chronic liver disease due to HCV infection (Lanford et al., 2001; Kremsdorf and Brezillon, 2007). However, use of chimpanzees is difficult from ethical and economical perspectives. The chimeric mouse with a humanized liver on the genetic background of urokinase plasminogen activator-transgenic severe combined immunodeficiency disorder (uPA/SCID) mice, designated as the PXB mouse, has been developed and characterized (Tateno et al., 2004). The livers of these mice are near completely (>70%) replaced with human hepatocytes and maintain the hepatic expression of most human drug-metabolizing enzymes and transporters (Nishimura et al., 2005). Subsequent studies have demonstrated that this mouse model is permissive to the infection of HCV in vivo and has potential utility in the discovery and development of new anti-HCV therapy (Umehara et al., 2006; Hiraga et al., 2007; Inoue et al., 2007). However, one should note that HCV-infected PXB mice do not precisely mimic chronic HCV infection in humans because these mice lack the adaptive immune response and liver disease associated with HCV infection as a result of their genetic background (SCID).

Because the primary organ of HCV infection and its replication is the liver, it is of great importance to know the possible alterations in the hepatic expression and activity of pharmacokinetics-related genes, i.e., drug transporters and metabolizing enzymes, by HCV infection. The aim of the present study was thus to investigate the effect of HCV infection on the mRNA expression of human ABC and SLC transporters and cytochrome P450 enzymes in the livers of PXB mice. Furthermore, the enzymatic activities of major human cytochrome P450 enzymes were compared between noninfected and HCV-infected PXB mice.

Materials and Methods

Generation of PXB Mice. PXB mice were generated by transplanting 1.0×10^6 human hepatocytes into the spleens of 2- to 3-week-old uPA/SCID mice under diethyl ether anesthesia as described previously (Tateno et al., 2004). All PXB mice used in the present study were derived from the same donor human hepatocyte (BD87, male, 2-year-old white; BD Biosciences, San Jose, CA).

Inoculation of HCV to PXB Mice. The inoculum used in the present study was HCV genotype 1b (HCR6, accession no. AY045702), which was obtained from HCV-infected PXB mice at the third passage. The original inoculum was obtained from the serum of an HCV-positive patient. PXB mice with a human albumin concentration in the blood greater than 6.0 mg/ml were infected with HCV genotype 1b at 9 to 10 weeks of age by injecting the inoculum (1.0×10^4 copies/mouse) to the retro-orbital sinus under diethyl ether anesthesia.

Quantification of Human Albumin Concentration and HCV Titer in the Serum. The concentration of human albumin in mouse blood was determined by latex agglutination immunonephelometry at 13 to 17 weeks of age. The replacement index is defined as the percentage of human hepatocyte repopulated in the host mouse liver and can be estimated from the blood human albumin value. RNA was extracted from the serum of PXB mice using a Sepa Gene RV-R RNA extraction system (Sanko Junyaku Co., Ltd., Ibaraki, Japan) according to the manufacturer's instructions, and the serum titer of HCV was determined by real-time quantitative PCR using TaqMan EZ RT-PCR Core Reagent and an ABI Prism 7500 sequence detector system as described previously (Takeuchi et al., 1999).

RNA Isolation and TaqMan Gene Expression Assays. Body weight was measured, and the liver was harvested from each mouse at 17 to 19 weeks of age. Total RNA was isolated from liver specimens using TRIzol (Invitrogen, Carlsbad, CA) according to the manufacturer's instructions and then treated with DNase I to remove contaminating genomic DNA. For cDNA synthesis, 80 ng of RNA was reverse-transcribed using a Transcriptor First Strand cDNA Synthesis Kit (Roche Applied Science, Indianapolis, IN) with random hexamer as the primer. The mRNA expression of human ABC transporters, SLC transporters, cytochrome P450 enzymes, and interferon-stimulated genes (ISGs) was quantified by TaqMan Gene Expression Assays on an ABI Prism 7900 system (Applied Biosystems, Foster City, CA) using LightCycler 480 Probe Master (Roche Applied Science) with primers and FAM-TAMRA or FAM-Iowa Black dual-labeled probes (Integrated DNA Technologies, Inc., Coralville, IA) that are specific for human genes. The protocol for PCR was as follows: 50°C for 2 min, 95°C for 10 min, and 40 cycles of 95°C for 15 s and 60°C for 1 min. The assay identification number or sequences of primers and probes used in the present study are listed in Table 1. The specificities of primers and probes to human genes were confirmed by comparing the amplification from human or mouse liver cDNA. No specific amplification was observed when mouse liver cDNA was used as a PCR template for all genes tested (data not shown). HCV RNA content in the livers of PXB mice was also quantified by TaqMan Gene Expression Assays using a cocktail of three forward primers, one reverse primer, and two TaqMan probes (Table 1) as described previously (Cook et al., 2004). The mRNA expression of each gene was quantified using the comparative C_t method, and normalized by the mRNA expression of hGAPDH.

Preparation of Liver Microsomes and Determination of Activities of Cytochrome P450 Enzymes. The microsomal fractions were isolated from the livers of noninfected and HCV-infected PXB mice at 18 or 20 weeks of age as described previously and stored at −70°C until further use (Sugihara et al., 2001). The activities of various P450s were determined in liver microsomes of PXB mice using selective substrates for the human P450 isoforms at appropriate concentrations (Table 2). In brief, 0.2 mg/ml microsomes were preincubated with substrate in 50 mM potassium phosphate buffer (pH 7.4) containing 5 mM $MgCl_2$ at 37°C for 5 min, and, subsequently, 2 mM NADPH was added to start the enzyme reaction. After the incubation at 37°C for 30 min (CYP1A2, CYP2C9, and CYP2C19), 15 min (CYP2D6), or 10 min (CYP3A4), the reaction was terminated by the addition of 150 μl of acetonitrile containing 7-hydroxycoumarin as an internal standard to 100 μl of incubation mixture. Samples were then centrifuged at 3000 rpm for 10 min at 4°C to precipitate the protein, and 10 μl of supernatant was analyzed by liquid chromatography (LC)-tandem mass spectrometry (MS/MS) to quantify the formation of metabolite. For the detection of acetaminophen, the supernatant as well as standard curves were further diluted with 5 mM ammonium acetate to ensure that the signal of each analyte was within the linear range of LC-MS/MS analysis. All of the experiments were conducted in triplicate.

LC-MS/MS Analysis. LC-MS/MS was performed on a Shimadzu high-performance liquid chromatography system with two LC-10ADvp pumps and the SCL-10Avp controller (Shimadzu Scientific Instruments, Columbia, MD) and an ABI Sciex API 4000 (Applied Biosystems). Samples were separated on a Hypersil BDS C18 column (50 × 2.1 mm, 5 μm; Thermo Fisher Scientific, Waltham, MA) with mobile phase A (0.1% formic acid in 5 mM ammonium acetate) and B (0.1% formic acid in acetonitrile/methanol 50/50, v/v) at a flow rate of 0.4 ml/min. High-performance liquid chromatography gradient programs were as follows: for CYP1A2, CYP2C9, and CYP2C19 assays,

TABLE 1

Assay identification number or sequences of primers and probes used for the TaqMan gene expression assays

Gene Name	RefSeq Identification	Assay Identification	Sequences (5′ to 3′)		
			Forward Primer	Reverse Primer	Probe
ABC transporters					
P-gp	NM_000927	Hs01067802_m1			
MDR3	NM_000443		CATCAATGACACCACTGAACTCAA	AACCTTGTCACCAATTCCTTCAC	CGCGGCTAACAGATGACATCTCCAAAA
BSEP	NM_003742		GGGCCATTGTACGAGATCCTAA	TGCACCGTCTTTTCACTTTCTG	TCTTGCTACTAGATGAAGCCACTTCTGCCTTAGA
MRP1	NM_004996		CATCGTGCAGGCGAGTGT	TCCTCACGGTGATGCTGTTC	TGACAGCATCGAGCGACGGCC
MRP2	NM_000392	Hs00166123_m1			
MRP3	NM_003786	Hs00358656_m1			
MRP4	NM_005845	Hs00195260_m1			
BCRP	NM_004827		CAGGTCTGTTGGTCAATCTCACA	TCCATATCGTGGAATGCTGAAG	CCATTGCATCTTGGCTGTCATGGCTT
SLC transporters					
NTCP	NM_003049		CCATGACACCACTCTTGATTGC	CGTCTGCACCGTCCATTG	ACCTCCTCCCTGATGCCTTTTATTGGC
OCT1	NM_003057	Hs00427550_m1			
OAT2	NM_006672		CTGCTAGTGTCCTCCGATATGAAG	GCACCGTAGGGTACAACTCTGAA	AAGCTGCCTTCACCACTGCCTACCTG
OATP1B1	NM_006446		GTACCACTTTCTTATTGCAACTCAGACT	CAGGGTGAGATGTAAGTTATTCCATTG	TCCACAGACTGGTTCCCATTGACTTTCA
OATP1B3	NM_019844	Hs00251986_m1			
OATP2B1	NM_007256		TCCTGTTTGCAGTGACCATGA	CACCTTCTGGCATCTGGTTAATG	CAGCCTCATGCTGCGCCTTTATGTG
Cytochrome P450 enzymes					
CYP1A1	NM_000499		TGGTCAAGGAGCACTACAAAACC	AGGTCCAAGACGATGTTAATGATCT	ATGAGAACGCCAATGTCCAGCTGTCA
CYP1A2	NM_000761		GGAGACCTTCCGACACTCCTC	CGTTGTGTCCCTTGTTGTGC	TTCTTGCCCTTCACCATCCCCAC
CYP2A6	NM_000762	Hs00711162_s1			
CYP2B6	NM_000767		TTGTTCTACCAGACTTTTTCACTCATC	GGAAAGTATTTCAAGAAGCCAGAGA	TCTGTATTCGGCCAGCTGTTTGAGCTC
CYP2C8	NM_000770	Hs00426387_m1			
CYP2C9	NM_000771	Hs00426397_m1			
CYP2C18	NM_000772	Hs00426403_m1			
CYP2C19	NM_000769	Hs00426380_m1			
CYP2D6	NM_000106	Hs00164385_m1			
CYP2E1	NM_000773	Hs00559368_m1			
CYP3A4	NM_017460		CAGGAGGAAATTGATGCAGTTTTT	GTCAAGATACTCCATCTGTAGCACAGT	CCCAATAAGGCACCACCCACCTATGA
CYP3A5	NM_000777		TGGACTTTTTAAGAGACTGGGAATTC	AAATTTCCAGAGACCCTGACGAT	CACACCTCTGCCTTTGTTGGGAAATGTT
ISGs					
CIG5	NM_080657		AGATGTTTCTGAAGCGAGGA	GCAGACAATGGCAGTTACTC	TGGATTGGTAGAGCGGAAAGTGGA
G1P2	NM_005101		CTCATCTTTGCCAGTACAGG	AGCTCTGACACCGACAT	CCATGGGCTGGGACCTGACG
G1P3	NM_002038		AAGGCCCTGACCTTCAT	ATTCAGGATCGCAGACCA	AGGAGGACTCGCAGTCGCC
HSXIAPAF1	NM_017523		CTTGAGCACCAGCAGG	GCATGTCCAGTTTGCAGA	TCATAAGGCCAATGAGTGCCAGGA
IFI27	NM_005532		GTAGTTTTGCCCCTGGC	GACATCATCTTGGCTGCT	TGTGATTGGAGGAGTTGTGGCTGT
IFI35	NM_005533		CAAGATGAGGCTGTGGGA	AGACTTAGGCACTTCCGG	CCCCAAAGACAAGGTCCCATTTTCAG
IFI44	NM_006417		GCTACCCTCAGCTCTAGC	CGCTTCCCTCCAAAATGA	ACTGCCATACTTCTTGATCTGTTGTACTGT
IFIT2	NM_001547		AGGAAGATTTCTGAAGAGTGC	GTTCCAGGTGAAATGGCA	CACTGCAACCATGAGTGAGAACAATAAGAA
IFITM1	NM_003641		TCCTCATGACCATTGGATTCATC	CCGTTTTTCCTGTATTATCTGTAACATAA	AGACTGTCACAGAGCCGAATACCA
IRF7	NM_001572		GCAGCGTGAGGGTGTGTCTT	GGAAGCACTCGATGTCGTCAT	CCTGTCCAGCGCCAACAGCC
IRF9/ISGF3G	NM_006084	Hs00196051_m1			
MX1	NM_002462		AAGGAATGGGAATCAGTCATGAG	TCTATTAGAGTCAGATCCGGGACAT	CACCCTGGAGATCAGCTCCCGA
MX2	NM_002463		CTAGAGCTTCAGGACCCT	TGATGGTCAGGTCTGGAAC	CGTTCTGGGCTTTGTGTATCTCTTTCTC
OAS1	NM_016816		TGTGTGTCCAAGGTGGTAAAGG	CAACCAGGTCAGCGTCAGATC	CCTCAGGCAAGGGCACCACCCT
OAS2	NM_016817	Hs00942643_m1			
OAS3	NM_006187	Hs00196324_m1			
OASL	NM_003733	Hs00984390_m1			
SP110	NM_004510		CAAAGCGATGAGATCCTGAG	CTGAGTCTTCTTCCGCATTC	CTTGTCATTGGTCACTGAAGTGCTTCT
STAT1	NM_007315		GTGGAAAGACAGCCCTGCAT	ACTGGACCCCTGTCTTCAAGAC	AACGCACCCTCAGAGGCCGC
TLR3	NM_003265	Hs01551078_m1			
TNFSF10	NM_003810		TGCGTGCTGATCGTGATCTT	GTACTTGTCCTGCATCTGCTTCA	TGCTCCTGCAGTCTCTCTGTGTGGCT
TRIM22	NM_006074		GCAGGAGTTTGTGACCAA	AGAGGTTCTGTCAGGAGC	CCAAGGGAGCAGTGCAATGGATTT

aspet DRUG METABOLISM AND DISPOSITION DMD

TABLE 1—*Continued.*

Gene Name	RefSeq Identification	Assay Identification	Sequences (5′ to 3′)		
			Forward Primer	Reverse Primer	Probe
Others					
GAPDH	NM_002046		GAAGGTGAAGGTCGGAGTC	GAAGATGGTGATGGGATTTC	CAAGCTTCCCGTTCTCAGCC
HCV (5′-UTR)			GCGACACTCCACCATAGATCACT CGACACTCCACCATGAATCACT CACTCCGCCATGAAYCACT[a]	CACTCGCAAGCACCCTATCA	AGGCCTTTCGCGACCCAACACTACTC AGGCCTTTCGCAACCCAACGCTACT

UTR, untranslated region.
[a] Y = C or T.

1) mobile phase B was maintained at 5% for 1.0 min, 2) increased linearly to 90% from 1.0 to 2.0 min and maintained to 3.0 min, and 3) brought back to the initial concentration linearly from 3.0 to 3.1 min for reequilibration, total run time 4.0 min; for CYP2D6 assay, 1) mobile phase B was maintained at 5% for 1.0 min, 2) increased linearly to 95% from 1.0 to 2.0 min and maintained to 4.0 min, and 3) brought back to the initial concentration linearly from 4.0 to 4.1 min for reequilibration, total run time 6.0 min; and for CYP3A4 assay, 1) mobile phase B was maintained at 5% for 1.0 min, 2) increased linearly to 95% from 1.0 to 2.0 min and maintained to 3.0 min, and 3) brought back to the initial concentration linearly from 3.0 to 3.1 min for reequilibration, total run time 4.0 min. The MS/MS parameters and linear range of standard curves (limit of detection to maximum concentration) are listed for each metabolite in Table 2. Data were collected and processed using Sciex Analyst 1.4.2 data collection and integration software.

Statistical Analysis. Statistical analysis was performed by Student's *t* test using GraphPad Prism (version 4). Asterisks represent significant differences (*, $P < 0.05$, **, $P < 0.01$, and ***, $P < 0.001$, respectively) between noninfected and HCV-infected PXB mice.

Results

Human Albumin Concentration and HCV Titers in PXB Mice. Sex, human albumin concentration in the blood, body weight, serum HCV titers, and HCV RNA content in the liver are summarized in Table 3 for each mouse. The sex of PXB mice did not affect the activity of human cytochrome P450 enzymes derived from the human hepatocytes inside the host mouse liver (supplemental data). The average concentration of human albumin in the blood was not significantly different between noninfected and HCV-infected PXB mice. Accordingly, the replacement index of human hepatocytes estimated from the albumin concentration was similar between the two groups. Although body weight at the time of liver isolation was significantly higher in HCV-infected PXB mice than in noninfected mice for those used for the preparation of total liver RNA, the difference was not statistically significant in those used for the preparation of liver microsomes. Indeed, unpublished observations (C. Tateno) with different batches of HCV-infected mice suggested that HCV infection does not significantly affect the body weight of either male or female PXB mice. Serum HCV titers were determined in HCV-infected PXB mice, and HCV RNA content in the liver was measured in both noninfected and HCV-infected groups. A significant amount of HCV RNA was detected in both the serum and liver of HCV-infected mice, whereas HCV RNA was not detected in the liver of noninfected mice. These results confirmed that PXB mice were successfully infected by HCV.

Activation of Interferon-Signaling Pathways in HCV-Infected PXB Mice. Previous reports suggested that chronic infection with HCV is accompanied by the up-regulation of genes related to the interferon-signaling pathways in human patients (Smith et al., 2006). To corroborate the relevance of our experimental model in PXB mice to clinical HCV infection, the mRNA expression of human ISGs observed to be activated in HCV-infected patients was quantified in the livers of noninfected and HCV-infected mice. Fourteen of 22 ISGs investigated exhibited a significant increase in mRNA expression in the livers of HCV-infected PXB mice compared with that in noninfected mice (Fig. 1). The mRNA expression of MX2 was below the limit of detection in both groups. These results suggest that the interferon signaling pathways are activated by HCV infection in PXB mice, which is similar to what is observed in patients with chronic HCV infection.

mRNA Expression of Human ABC and SLC Transporters. The mRNA expression of major human hepatic ABC and SLC transporters was quantified in the livers of noninfected and HCV-infected PXB mice (Fig. 2). A significant increase in mRNA expression was ob-

TABLE 2

Substrate concentration and analytical parameters for each metabolite in MS/MS

Enzyme	Substrate	Metabolite	Mass Transition (*m/z*)	Mode	CE	DP	Linear Range
					eV	*eV*	
CYP1A2	Phenacetin (10 μM)	Acetaminophen	152.13 > 110.15	ESI+	22	46	10 nM–10 μM
CYP2C9	Diclofenac (5 μM)	4′-Hydroxydiclofenac	312.09 > 230.01	ESI+	45	41	1 nM–1 μM
CYP2C19	(*S*)-Mephenytoin (50 μM)	4′-Hydroxymephenytoin	235.10 > 150.21	ESI+	24	56	1 nM–1 μM
CYP2D6	Dextromethorphan (5 μM)	Dextrorphan	258.17 > 157.10	ESI+	51	81	1 nM–1 μM
CYP3A4	Midazolam (1 μM)	1′-Hydroxymidazolam	341.82 > 203.20	ESI+	38	71	1 nM–1 μM

CE, collision energy; DP, declustering potential; ESI, electrospray ionization.

TABLE 3

Human albumin concentration, estimated replacement index, body weight, and HCV content in the serum and liver of PXB mice

Animal	Sex	h-Alb	Estimated RI	Body Weight	Serum HCV Titer (10^7 copies/ml)	HCV RNA Content in the Liver (Relative to hGAPDH)
		mg/ml	%	*g*		
PXB mice used for the preparation of total liver RNA						
Noninfected						
PXB41-18	Male	6.3	74.2	14.4	—[a]	N.D.
PXB41-25	Male	8.2	82.3	13.7	—	N.D.
PXB42-1	Male	12.2	94.6	15.0	—	N.D.
Mean ± S.D.		8.9 ± 3.0	83.7 ± 10.3	14.3 ± 0.6	—	—
HCV-infected						
PXB36-11	Male	5.3	68.9	17.2	5.15	4.95×10^{-3}
PXB36-23	Male	7.7	80.4	16.8	5.52	3.53×10^{-3}
PXB38-11	Male	5.8	71.7	16.2	2.12	3.16×10^{-3}
Mean ± S.D.		6.3 ± 1.3	73.7 ± 6.0	16.7 ± 0.5*	4.26 ± 1.87	$3.88 \times 10^{-3} \pm 9.46 \times 10^{-4}$
PXB mice used for the preparation of liver microsomes						
Noninfected						
PXB22-47	Female	6.3	74.2	19.8	—	—
PXB22-48	Female	7.3	78.7	11.5	—	—
PXB22-57	Female	5.2	68.2	14.7	—	—
Mean ± S.D.		6.3 ± 1.1	73.7 ± 5.3	15.3 ± 4.2	—	—
HCV-infected						
PXB86-13	Male	6.3	74.2	22.8	6.56	—
PXB86-26	Female	3.5	55.9	19.4	0.806	—
PXB86-33	Male	6.4	74.6	22.1	4.66	—
Mean ± S.D.		5.4 ± 1.6	68.2 ± 10.7	21.4 ± 1.8	4.01 ± 2.93	—

h-Alb, human albumin; RI, replacement index; N.D., not detected.
* $P < 0.01$, significantly different between noninfected and HCV-infected PXB mice.
[a] —, not determined.

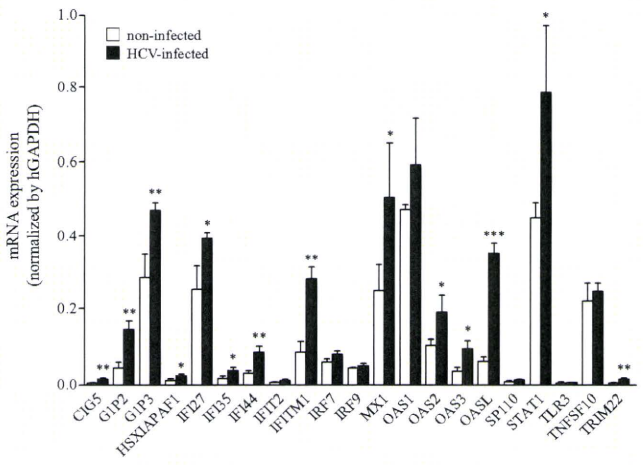

FIG. 1. Activation of interferon signaling pathways in HCV-infected PXB mice. The mRNA expression of human interferon-stimulated genes was measured in the livers of noninfected and HCV-infected PXB mice by TaqMan Gene Expression Assays as described under *Materials and Methods*, and the data were normalized by the mRNA expression of hGAPDH. Results are presented as the mean ± S.D. of three mice. □, mRNA expression in noninfected PXB mice; ■, mRNA expression in HCV-infected PXB mice. *, $P < 0.05$; **, $P < 0.01$; ***, $P < 0.001$, significantly different between noninfected and HCV-infected mice.

served for MRP4 and OATP2B1 in HCV-infected PXB mice compared with that in noninfected mice. In contrast, OCT1 was significantly decreased in HCV-infected PXB mice compared with that in their noninfected controls. The mRNA expression of MRP1 was below the limit of detection in both noninfected and HCV-infected groups. The mRNA levels of other ABC and SLC transporters, including P-gp, MDR3, BSEP, MRP2, MRP3, NTCP, OAT2, OATP1B1, and OATP1B3, were comparable between the two groups.

mRNA Expression of Human Cytochrome P450 Enzymes. The mRNA expression of 12 human cytochrome P450 genes, *CYP1A1*, *CYP1A2*, *CYP2A6*, *CYP2B6*, *CYP2C8*, *CYP2C9*, *CYP2C18*, *CYP2C19*, *CYP2D6*, *CYP2E1*, *CYP3A4*, and *CYP3A5*, was investigated in the livers of noninfected and HCV-infected PXB mice (Fig. 3). The mRNA expression of these genes was not statistically different between the two groups with the exception of significantly lower expression of CYP2D6 in HCV-infected mice.

Activity of Human Cytochrome P450 Enzymes. The activities of five major human cytochrome P450 enzymes, namely, CYP1A2, CYP2C9, CYP2C19, CYP2D6, and CYP3A4, were investigated in the liver microsomes of noninfected and HCV-infected PXB mice (Fig. 4). The metabolic activity in the liver microsomes from uPA/SCID mice for each probe substrate was comparable to or lower than that in human liver microsomes (C. Tateno, unpublished observations). Taking into account the fact that the livers of PXB mice are nearly completely (>70%) replaced with human hepatocytes, the background activity from remaining mouse hepatocyte in PXB

DRUG METABOLISM AND DISPOSITION DMD aspet

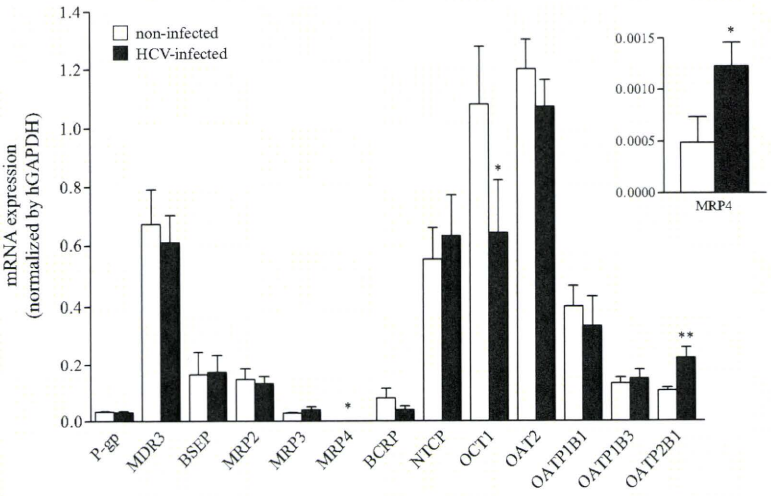

FIG. 2. mRNA expression profiles of drug transporters in PXB mice. The mRNA expression of human ABC and SLC transporters was measured in the livers of noninfected (□) and HCV-infected (■) PXB mice by TaqMan Gene Expression Assays, and the data are presented as described in the legend to Fig. 1. The inset represents the magnification of the mRNA expression of MRP4.

mice is minor. The metabolic activity of CYP1A2 was significantly lower in HCV-infected PXB mice than in noninfected PXB mice. The activities of other P450s were similar between noninfected and HCV-infected PXB mice.

Discussion

In the present study, the effect of HCV infection on the mRNA expression profiles of human ABC and SLC transporters and cytochrome P450 enzymes in PXB mice was investigated. The primers and probes specific for human genes were used in the TaqMan gene expression assays to exclude the background amplification of homologous genes from the host mouse liver. In addition, we have characterized enzymatic activities of major human P450s in the microsomes isolated from the livers of PXB mice.

The body weight and human albumin concentration in the blood of PXB mice were similar between noninfected and HCV-infected groups, suggesting that the inoculation of HCV does not affect the growth of transplanted human hepatocytes inside the host mouse liver or maturation of the mice (Table 3). A profound effect of HCV infection was observed on the status of interferon-signaling pathways, for which mRNA expression of a series of ISGs was significantly higher in the livers of HCV-infected PXB mice compared with that of noninfected controls (Fig. 1). The up-regulation of ISGs are in good agreement with the observation in patients with chronic HCV infection and chimpanzees with acute HCV infection (Su et al., 2002; Smith et al., 2006). In addition, these data are similar to the results published previously by Walters et al. (2006) who also used the human hepatocyte chimeric mouse model to examine the regulation of overall hepatic gene expression by HCV genotype 1a infection with microarray technology. It is of note that the effect of HCV infection on the expression of ISGs was comparable between genotype 1a (Walters et al., 2006) and 1b (this study). It is likely that there is no marked difference between the two HCV genotypes in terms of their effects on gene expression. It has been previously demonstrated that viremia in PXB mice can be reduced by treatment with IFN-α or pegylated-IFN as in human patients (Umehara et al., 2006; Hiraga et al., 2007; Inoue et al., 2007). The presence of functional interferon signaling pathways in PXB mice, suggested by the up-regulation of a number of ISGs by HCV infection, provides a rationale for the efficacy of those antiviral agents in this model. These observations warrant the use of PXB mice as an in vivo model for the primary infection of the liver by HCV to investigate the effects of novel anti-HCV compounds on suppressing the replication of HCV.

There were, in general, few marked differences in the mRNA expression of human ABC and SLC transporters and cytochrome P450 enzymes in the liver between noninfected and HCV-infected PXB mice with some exceptions, e.g., significantly higher expression

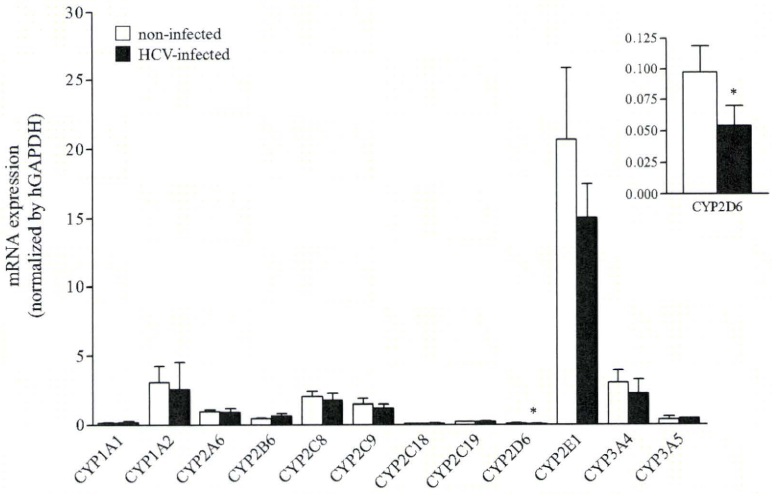

FIG. 3. mRNA expression profiles of drug-metabolizing enzymes in PXB mice. The mRNA expression of human cytochrome P450 enzymes was measured in the livers of noninfected (□) and HCV-infected (■) PXB mice by TaqMan Gene Expression Assays, and the data are presented as described in the legend to Fig. 1. The inset represents the magnification of the mRNA expression of CYP2D6.

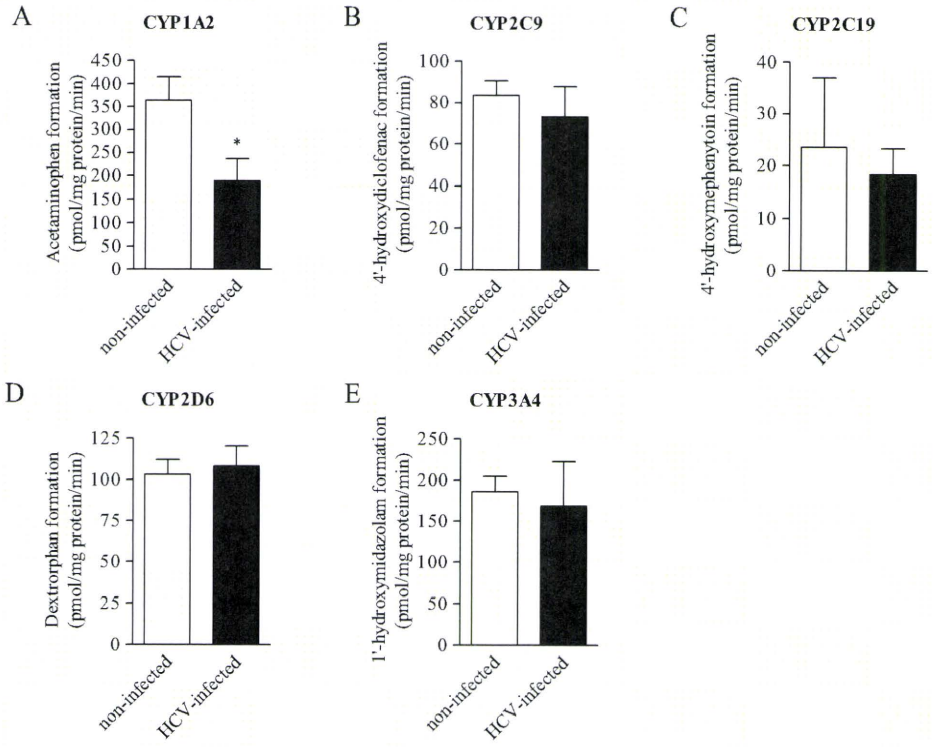

FIG. 4. Activity of human cytochrome P450 enzymes in PXB mice. The activities of five major human cytochrome P450 enzymes, i.e., CYP1A2 (A), CYP2C9 (B), CYP2C19 (C), CYP2D6 (D), and CYP3A4 (E), were measured in the liver microsomes of noninfected and HCV-infected PXB mice as described under *Materials and Methods*. Results are presented as the mean ± S.D. of three mice. □, metabolic activity in noninfected PXB mice; ■, metabolic activity in HCV-infected PXB mice. *, $P < 0.05$, significantly different between noninfected and HCV-infected mice.

of MRP4 and OATP2B1 and lower expression of OCT1 and CYP2D6 in HCV-infected mice than in noninfected mice (Figs. 2 and 3). Likewise, the activities of major human cytochrome P450 enzymes were similar between noninfected and HCV-infected PXB mice except for CYP1A2, which exhibited a significantly lower activity in HCV-infected PXB mice than in noninfected mice (Fig. 4). The effect of HCV infection on the mRNA expression and enzymatic activity of CYP1A2 and CYP2D6 was not consistent. The change in mRNA expression of CYP2D6 might not be sufficient to affect its enzymatic activity, whereas posttranscriptional effects of HCV infection may explain the decreased enzymatic activity of CYP1A2 regardless of unchanged mRNA expression. In consideration of the induction of many ISGs at the mRNA level, it is likely that the effect of HCV infection on the expression of pharmacokinetics-related genes would also be observed, if any, at the transcriptional level (CYP1A2 might be an exception). HCV infection probably affects gene expression via direct interference by virus infection, that is, the innate antiviral response and/or indirect interference by adaptive HCV-specific immune response, oxidative stress, and liver disease associated with chronic infection (Pawlotsky, 1998; Missale et al., 2004). PXB mice are immunocompromised because of their genetic background and thus lack the adaptive immune response and liver disease associated with HCV infection: i.e., there was no hepatocyte damage or inflammation in the liver of infected chimeric mice (Hiraga et al., 2007). HCV infection will thus affect gene expression only through the innate antiviral response in our experimental model. The similar expression profiles of drug transporters and metabolizing enzymes between noninfected and HCV-infected PXB mice suggest that innate antiviral signaling pathways play only a minor role in the regulation of mRNA expression of these genes.

There have been several reports regarding the aberrant mRNA expression of drug transporters and metabolizing enzymes in patients with HCV infection compared with those without infection or healthy volunteers. Hinoshita et al. (2001) have demonstrated that the mRNA expression of P-gp, MDR3, MRP1, MRP2, and MRP3 in the noncancerous region in the liver of patients with hepatic tumor tends to be lower in HCV-infected groups than in noninfected ones. On the other hand, Ros et al. (2003) have reported increased mRNA expression of P-gp and MRP3 in the livers of patients with HCV infection compared with healthy volunteers, whereas there was no significant difference for MRP2. Nakai et al. (2001) have performed a comprehensive study of variation in the mRNA levels of drug transporters and metabolizing enzymes in patients with chronic hepatitis C using quantitative real-time PCR and observed clear correlations between fibrosis stage and mRNA levels of CYP1A2, CYP2E1, CYP3A4, NTCP, OCT1, and OATP1B1 in the liver, whereas no fibrosis stage-dependent differences were observed for other transporters and enzymes that included P-gp, MDR3, MRP1, MRP2, and MRP3 (Nakai et al., 2008). Intriguingly, these clinical observations are inconsistent with the present findings in PXB mice in which HCV infection affects gene expression primarily through the innate antiviral response. The altered expression of drug transporters and metabolizing enzymes in clinical patients might be ascribed to the indirect interference by HCV infection or secondary effects as a result of the development of liver fibrosis or other hepatic dysfunction resulting from HCV infection. Indeed, serum levels or spontaneous productions by peripheral blood mononuclear cells of inflammatory cytokines such as tumor necrosis factor-α, interleukin-1β, and interleukin-6 were elevated in HCV-infected patients compared with those in healthy subjects (Kishihara et al., 1996; Huang et al., 1999; Cotler et al., 2001). In addition, several lines of evidence suggest perturbation of the expression of drug transporters and metabolizing enzymes by these cytokines both in vivo and in vitro (Lee and Piquette-Miller, 2003; Geier et al., 2005; Renton, 2005; Vee et al., 2009). Oxidative stress and liver diseases including cirrhosis and hepatocellular carcinoma, which are prevalent in patients with chronic HCV infection, also compromise the physiological expression of drug transporters (Bonin et al., 2002; Toyoda et al., 2008). This complex nature of HCV infection and progression to liver disease may

account for the controversial findings regarding the expression of pharmacokinetics-related genes in clinical patients with HCV infection, although the possibility of a difference in the patient population cannot be ruled out.

Because all PXB mice used in the present study are derived from a single donor hepatocyte, future studies are necessary to generalize the present findings by characterizing different batches of PXB mice originated from other donor hepatocytes. Nevertheless, the present study has clearly demonstrated that the infection of PXB mice, the chimeric mice with humanized liver, by HCV triggers the activation of interferon-signaling pathways as observed in human patients with chronic infection, but in general does not have a significant impact on the mRNA expression profiles of human ABC and SLC transporters or on the mRNA expression and enzymatic activity of cytochrome P450 enzymes. These results suggest that the pharmacokinetic behavior of small molecule antiviral therapies such as protease and polymerase inhibitors is likely to be comparable between HCV-infected and noninfected PXB mice. The PXB mouse model is a good model to study the effects of novel anti-HCV compounds in the primary treatment of HCV infection on suppressing the replication of HCV and therefore to investigate the relationship of the pharmacokinetics and pharmacodynamics of such therapies. However, caution is needed in the translation of this relationship to HCV-infected patients because PXB mice are immunocompromised based on their genetic background (SCID), and thus this mouse model does not accurately reflect the liver disease and immune response such as the increase in the levels of inflammatory cytokines observed in patients with chronic HCV infection, which may lead to changes in drug transporter and metabolizing enzyme expression.

Acknowledgments. We thank Drs. Yasuhisa Adachi and Shin-ichi Ninomiya for their technical assistance in the microsome assays.

References

Bartenschlager R (2005) The hepatitis C virus replicon system: from basic research to clinical application. *J Hepatol* **43:**210–216.

Bonin S, Pascolo L, Crocé LS, Stanta G, and Tiribelli C (2002) Gene expression of ABC proteins in hepatocellular carcinoma, perineoplastic tissue, and liver diseases. *Mol Med* **8:**318–325.

Buck M (2008) Direct infection and replication of naturally occurring hepatitis C virus genotypes 1, 2, 3 and 4 in normal human hepatocyte cultures. *PLoS One* **3:**e2660.

Chandra P and Brouwer KL (2004) The complexities of hepatic drug transport: current knowledge and emerging concepts. *Pharm Res* **21:**719–735.

Cook L, Ng KW, Bagabag A, Corey L, and Jerome KR (2004) Use of the MagNA pure LC automated nucleic acid extraction system followed by real-time reverse transcription-PCR for ultrasensitive quantitation of hepatitis C virus RNA. *J Clin Microbiol* **42:**4130–4136.

Cotler SJ, Reddy KR, McCone J, Wolfe DL, Liu A, Craft TR, Ferris MW, Conrad AJ, Albrecht J, Morrissey M, Ganger DR, Rosenblate H, Blatt LM, Jensen DM, and Taylor MW (2001) An analysis of acute changes in interleukin-6 levels after treatment of hepatitis C with consensus interferon. *J Interferon Cytokine Res* **21:**1011–1019.

Dobson PD and Kell DB (2008) Carrier-mediated cellular uptake of pharmaceutical drugs: an exception or the rule? *Nat Rev Drug Discov* **7:**205–220.

Geier A, Dietrich CG, Voigt S, Ananthanarayanan M, Lammert F, Schmitz A, Trauner M, Wasmuth HE, Boraschi D, Balasubramaniyan N, Suchy FJ, Matern S, and Gartung C (2005) Cytokine-dependent regulation of hepatic organic anion transporter gene transactivators in mouse liver. *Am J Physiol Gastrointest Liver Physiol* **289:**G831–G841.

Gonzalez FJ (1990) Molecular genetics of the P-450 superfamily. *Pharmacol Ther* **45:**1–38.

Hinoshita E, Taguchi K, Inokuchi A, Uchiumi T, Kinukawa N, Shimada M, Tsuneyoshi M, Sugimachi K, and Kuwano M (2001) Decreased expression of an ATP-binding cassette transporter, MRP2, in human livers with hepatitis C virus infection. *J Hepatol* **35:**765–773.

Hiraga N, Imamura M, Tsuge M, Noguchi C, Takahashi S, Iwao E, Fujimoto Y, Abe H, Maekawa T, Ochi H, Tateno C, Yoshizato K, Sakai A, Sakai Y, Honda M, Kaneko S, Wakita T, and Chayama K (2007) Infection of human hepatocyte chimeric mouse with genetically engineered hepatitis C virus and its susceptibility to interferon. *FEBS Lett* **581:**1983–1987.

Huang YS, Hwang SJ, Chan CY, Wu JC, Chao Y, Chang FY, and Lee SD (1999) Serum levels of cytokines in hepatitis C-related liver disease: a longitudinal study. *Zhonghua Yi Xue Za Zhi (Taipei)* **62:**327–333.

Inoue K, Umehara T, Ruegg UT, Yasui F, Watanabe T, Yasuda H, Dumont JM, Scalfaro P, Yoshiba M, and Kohara M (2007) Evaluation of a cyclophilin inhibitor in hepatitis C virus-infected chimeric mice in vivo. *Hepatology* **45:**921–928.

Kishihara Y, Hayashi J, Yoshimura E, Yamaji K, Nakashima K, and Kashiwagi S (1996) IL-1β and TNF-α produced by peripheral blood mononuclear cells before and during interferon therapy in patients with chronic hepatitis C. *Dig Dis Sci* **41:**315–321.

Kremsdorf D and Brezillon N (2007) New animal models for hepatitis C viral infection and pathogenesis studies. *World J Gastroenterol* **13:**2427–2435.

Lanford RE, Bigger C, Bassett S, and Klimpel G (2001) The chimpanzee model of hepatitis C virus infections. *ILAR J* **42:**117–126.

Lee G and Piquette-Miller M (2003) Cytokines alter the expression and activity of the multidrug resistance transporters in human hepatoma cell lines; analysis using RT-PCR and cDNA microarrays. *J Pharm Sci* **92:**2152–2163.

Littlejohn M, Locarnini S, and Bartholomeusz A (1998) Targets for inhibition of hepatitis C virus replication. *Antivir Ther* **3:**83–91.

Meyer UA (1996) Overview of enzymes of drug metabolism. *J Pharmacokinet Biopharm* **24:**449–459.

Missale G, Cariani E, and Ferrari C (2004) Role of viral and host factors in HCV persistence: which lesson for therapeutic and preventive strategies? *Dig Liver Dis* **36:**703–711.

Nakai K, Tanaka H, Hanada K, Ogata H, Suzuki F, Kumada H, Miyajima A, Ishida S, Sunouchi M, Habano W, Kamikawa Y, Kubota K, Kita J, Ozawa S, and Ohno Y (2008) Decreased expression of cytochromes P450 1A2, 2E1, and 3A4 and drug transporters Na^+-taurocholate-cotransporting polypeptide, organic cation transporter 1, and organic anion-transporting peptide-C correlates with the progression of liver fibrosis in chronic hepatitis C patients. *Drug Metab Dispos* **36:**1786–1793.

Nishimura M, Yoshitsugu H, Yokoi T, Tateno C, Kataoka M, Horie T, Yoshizato K, and Naito S (2005) Evaluation of mRNA expression of human drug-metabolizing enzymes and transporters in chimeric mouse with humanized liver. *Xenobiotica* **35:**877–890.

Pawlotsky JM (1998) Hepatitis C virus infection: virus/host interactions. *J Viral Hepat* **5(Suppl 1):**3–8.

Rendic S and Di Carlo FJ (1997) Human cytochrome P450 enzymes: a status report summarizing their reactions, substrates, inducers, and inhibitors. *Drug Metab Rev* **29:**413–580.

Renton KW (2005) Regulation of drug metabolism and disposition during inflammation and infection. *Expert Opin Drug Metab Toxicol* **1:**629–640.

Ros JE, Libbrecht L, Geuken M, Jansen PL, and Roskams TA (2003) High expression of MDR1, MRP1, and MRP3 in the hepatic progenitor cell compartment and hepatocytes in severe human liver disease. *J Pathol* **200:**553–560.

Shitara Y, Horie T, and Sugiyama Y (2006) Transporters as a determinant of drug clearance and tissue distribution. *Eur J Pharm Sci* **27:**425–446.

Smith MW, Walters KA, Korth MJ, Fitzgibbon M, Proll S, Thompson JC, Yeh MM, Shuhart MC, Furlong JC, Cox PP, Thomas DL, Phillips JD, Kushner JP, Fausto N, Carithers RL Jr, and Katze MG (2006) Gene expression patterns that correlate with hepatitis C and early progression to fibrosis in liver transplant recipients. *Gastroenterology* **130:**179–187.

Su AI, Pezacki JP, Wodicka L, Brideau AD, Supekova L, Thimme R, Wieland S, Bukh J, Purcell RH, Schultz PG, and Chisari FV (2002) Genomic analysis of the host response to hepatitis C virus infection. *Proc Natl Acad Sci USA* **99:**15669–15674.

Sugihara K, Kitamura S, Yamada T, Ohta S, Yamashita K, Yasuda M, and Fujii-Kuriyama Y (2001) Aryl hydrocarbon receptor (AhR)-mediated induction of xanthine oxidase/xanthine dehydrogenase activity by 2,3,7,8-tetrachlorodibenzo-*p*-dioxin. *Biochem Biophys Res Commun* **281:**1093–1099.

Takeuchi T, Katsume A, Tanaka T, Abe A, Inoue K, Tsukiyama-Kohara K, Kawaguchi R, Tanaka S, and Kohara M (1999) Real-time detection system for quantification of hepatitis C virus genome. *Gastroenterology* **116:**636–642.

Tateno C, Yoshizane Y, Saito N, Kataoka M, Utoh R, Yamasaki C, Tachibana A, Soeno Y, Asahina K, Hino H, Asahara T, Yokoi T, Furukawa T, and Yoshizato K (2004) Near completely humanized liver in mice shows human-type metabolic responses to drugs. *Am J Pathol* **165:**901–912.

Toyoda Y, Hagiya Y, Adachi T, Hoshijima K, Kuo MT, and Ishikawa T (2008) MRP class of human ATP binding cassette (ABC) transporters: historical background and new research directions. *Xenobiotica* **38:**833–862.

Umehara T, Sudoh M, Yasui F, Matsuda C, Hayashi Y, Chayama K, and Kohara M (2006) Serine palmitoyltransferase inhibitor suppresses HCV replication in a mouse model. *Biochem Biophys Res Commun* **346:**67–73.

Vee ML, Lecureur V, Stieger B, and Fardel O (2009) Regulation of drug transporter expression in human hepatocytes exposed to the proinflammatory cytokines tumor necrosis factor-α or interleukin-6. *Drug Metab Dispos* **37:**685–693.

Wakita T (2007) HCV research and anti-HCV drug discovery: toward the next generation. *Adv Drug Deliv Rev* **59:**1196–1199.

Wakita T (2006) Host-specific response to HCV infection in the chimeric SCID-beige/Alb-uPA mouse model: role of the innate antiviral immune response. *PLoS Pathog* **2:**e59.

Williams JA, Hyland R, Jones BC, Smith DA, Hurst S, Goosen TC, Peterkin V, Koup JR, and Ball SE (2004) Drug-drug interactions for UDP-glucuronosyltransferase substrates: a pharmacokinetic explanation for typically observed low exposure (AUCi/AUC) ratios. *Drug Metab Dispos* **32:**1201–1208.

World Health Organization (1999) Global surveillance and control of hepatitis C. Report of a WHO Consultation organized in collaboration with the Viral Hepatitis Prevention Board, Antwerp, Belgium. *J Viral Hepat* **6:**35–47.

Address correspondence to: Dr. Adrian J. Fretland, Hoffmann-La Roche, 340 Kingsland St., Bldg. 123/1331, Nutley, NJ 07110-1199. E-mail: adrian.fretland@roche.com

Drug Metab. Pharmacokinet. 25 (6): 539–550 (2010).

Regular Article

In Vitro Evaluation of Cytochrome P450 and Glucuronidation Activities in Hepatocytes Isolated from Liver-Humanized Mice

Chihiro YAMASAKI[1,2], Miho KATAOKA[2], Yumiko KATO[1], Masakazu KAKUNI[1], Sadakazu USUDA[3], Yoshihiro OHZONE[4], Sunao MATSUDA[4], Yasuhisa ADACHI[4], Shin-ichi NINOMIYA[4], Toshiyuki ITAMOTO[5], Toshimasa ASAHARA[5], Katsutoshi YOSHIZATO[1,6] and Chise TATENO[1,2,*]

[1]*PhoenixBio, Co., Ltd., Higashihiroshima, Japan*
[2]*Cooperative Link of Unique Science and Technology for Economy Revitalization, Hiroshima Prefectural Institute of Industrial Science and Technology; Higashihiroshima, Japan*
[3]*Immunojapan Inc., Tokyo, Japan*
[4]*Sekisui Medical Inc., Tokai, Japan*
[5]*Hiroshima University, Graduate School of Biomedical Sciences, Division of Frontier Medical Science, Department of Surgery and Hiroshima University 21st Century COE Program for Advanced Radiation Casualty Medicine, Programs for Biomedical Research, Hiroshima, Japan*
[6]*Graduate School of Science, Hiroshima University, Higashihiroshima, Japan*

Full text of this paper is available at http://www.jstage.jst.go.jp/browse/dmpk

Summary: Cryopreserved human (h-) hepatocytes are currently regarded as the best *in vitro* model for predicting human intrinsic clearance of xenobiotics. Although fresh h-hepatocytes have greater plating efficiency on dishes and greater metabolic activities than cryopreserved cells, performing reproducible studies using fresh hepatocytes from the same donor and having an "on demand" supply of fresh hepatocytes are not possible. In this study, cryopreserved h-hepatocytes were transplanted into albumin enhancer/promoter-driven, urokinase-type plasminogen activator, transgenic/severe combined immunodeficient (uPA/SCID) mice to produce chimeric mice, the livers of which were largely replaced with h-hepatocytes. We determined whether the chimeric mouse could serve as a novel source of fresh h-hepatocytes for in vitro studies. h-Hepatocytes were isolated from chimeric mice (chimeric hepatocytes), and cytochrome P450 (P450) activities were determined. Compared with cryopreserved cells, the P450 (1A2, 2C9, 2C19, 2D6, 2E1, 3A) activities of fresh chimeric hepatocytes were similar or greater. Moreover, ketoprofen was more actively metabolized through glucuronide conjugates by fresh chimeric hepatocytes than by cryopreserved cells. We conclude that chimeric mice may be a useful tool for supplying fresh h-hepatocytes on demand that provide high and stable phase I enzyme and glucuronidation activities.

Keywords: human hepatocytes; chimeric mice; cytochrome P450; ketoprofen; UDP-glucuronosyltransferase

Introduction

"Chimeric mice" with livers repopulated with human hepatocytes (h-hepatocytes), created using urokinase-type plasminogen activator (uPA)/severe combined immunodeficient (SCID) mice,[1)] were previously established and the expression of both cytochrome P450 enzymes (P450s, CYPs) and phase II enzymes in the liver of these chimeric mice, as well as *in vivo* induction of P450, were examined.[1-4)]

P450 has been found to play an important role in the metabolism of xenobiotics, including drugs. Indeed, approximately 80% of oxidative metabolism is catalyzed by P450s,[5)] and to predict pharmacokinetics and drug interactions precisely, investigation of the pharmacokinetics of a P450 substrate using chimeric mice would be of considerable value.

Species differences are known to exist in the metabolism of ketoprofen.[6)] Ketoprofen is a propionic acid-class nonsteroidal anti-inflammatory drug with analgesic and

Received; May 17, 2010, Accepted; August 12, 2010, J-STAGE Advance Published Date; October 1, 2010
**To whom correspondence should be addressed:* Chise TATENO, Ph.D., *R&D Department, PhoenixBio, Co., Ltd., 3-4-1, Kagamiyama, Higashihiroshima, 739-0046, Japan. Tel/Fax. +81-82-431-0016, E-mail: chise.mukaidani@phoenixbio.co.jp*
This work was supported by CLUSTER and the Regional Science and Technology promotion budget.